Chapter 2

Physical Transport of Nutrients and the Maintenance of Biological Production

Richard G. Williams · Michael J. Follows

2.1 Introduction

The oceanic distributions of nutrients and patterns of biological production are controlled by the interplay of biogeochemical and physical processes, and external sources. Biological and chemical processes lead to the transformation of nutrients between inorganic and organic forms, and also between dissolved and particulate forms. Physical processes redistribute nutrients within the water column through transport and mixing. The combined role of biogeochemical and physical processes is reflected in the observed distributions of nitrate, phosphate and silicate (macro-nutrients). These distributions broadly reflect those of classical water masses, as defined by temperature and salinity, highlighting the important role of physical transport. However, there are also significant differences between the nutrient and water-mass distributions, notably with nutrients showing stronger vertical and basin-to-basin contrasts. Biological production leads to these greater nutrient contrasts with inorganic nutrients consumed and converted to organic matter in the surface, sunlit ocean. A small fraction of the organic matter in this euphotic zone is exported to depth, driven by the gravitational sinking of particles and subduction of dissolved organic matter. This organic fallout is eventually remineralised leading to an accumulation of inorganic nutrients in deeper and older water masses.

Biological production would eventually cease without other processes acting to supply nutrients to the surface ocean. This supply is largely achieved by ocean transport and mixing processes, redistributing nutrients within the water column, with some contribution from external inputs such as atmospheric deposition, river runoff in the coastal zone and nitrogen fixation. On long timescales, the external inputs are balanced by burial of organic nutrients in the sediments or denitrification. Traditionally, the physical transfer of nutrients from the deep to the surface ocean has been predominately viewed in terms of a vertical supply arising from large-scale vertical advection, diffusion and convection (Fig. 2.1a). Whether this picture holds outside upwelling zones depends on the strength of diapycnic mixing within the upper ocean. In order to explain the vertical profile of tracers, Munk (1966) diagnosed that the diabatic diffusivity needed to reach the order of 10^{-4} m^2 s^{-1}. However, direct observations of the mixing suggest that the diapycnic diffusivity is an order of magnitude smaller over much of the ocean interior, particularly in the subtropical thermocline[(1)]. Hence, such diffusive transfer is unlikely to dominate within the upper ocean or explain the nutrient supply to the euphotic zone.

Instead the maintenance of biological production is affected by the three-dimensional, time-varying circulation (Fig. 2.1b). The global-scale overturning plays a key role in transporting nutrients and modulating biological production. However, smaller-scale processes involving horizontal variations in convection, gyre circulations, boundary currents, eddies and fronts are also significant. For example, the spatial patterns of surface chlorophyll partly reflect those of physical processes, as shown later in Fig. 2.15 for a remotely-sensed view of the Gulf Stream.

Despite the important role of physical processes, there are significant differences in the individual nutrient and trace-metal distributions. For example, silicate differs from nitrate and phosphate distributions due to the relatively slow remineralisation of silica from sinking particles (Gnanadesikan 1998). Total nitrogen and phosphorus distributions become decoupled from each other through fixation of nitrogen gas at the surface and, perhaps, differential cycling of their dissolved organic forms (Wu et al. 2000). The processes controlling the distribution of iron, an important micronutrient, are not fully understood but appear to involve a combination of atmospheric deposition, geothermal inputs, and scavenging and complexation within the water column (e.g. Martin and Fitzwater 1988; Archer and Johnson 2000). Consequently, individual nutrients and trace metals have different distributions and each can be the limiting factor over different regions and at different times in the surface ocean (see a model illustration by Moore et al. 2002).

In this review, we address the following questions concerning the role of physical processes and their impact on biogeochemical cycling over the open ocean:

- How are observed nutrient distributions over global to kilometre scales controlled by physical transports and physical-biogeochemical interactions?
- What is the role of physical processes in maintaining and modulating biological productivity?
- How are the temporal variations in nutrient distributions and biological productivity, on interannual and longer timescales, connected to changes in atmospheric physical forcing and ocean circulation?

We adopt a mechanistic approach discussing the physical processes and their effect on biogeochemical cycles in the open ocean on horizontal scales ranging from global to frontal. The role of the overturning circulation is discussed in terms of the transport between ocean basins and the Southern Ocean. The role of convection is considered in terms of the seasonal cycle and its limited role in maintaining levels of export production. The role of gyres and boundary currents is outlined in terms of vertical and horizontal transports within ocean basins. The role of smaller-scale eddies and fronts is addressed in terms of both their local and far field transport effects. Finally, interannual and longer-term variability is discussed in terms of regional examples: the El Niño-Southern Oscillation, the North Atlantic Oscillation, the eastern Mediterranean and the glacial North Atlantic.

This review complements the reviews of Denman and Gargett (1995), who focussed on vertical and small-scale transport processes, and Barber (1992), who discussed large-scale processes and the geological record. For a more complete description of ocean circulation, modeling and data analysis, see contributions in the WOCE book edited by Siedler et al. (2001).

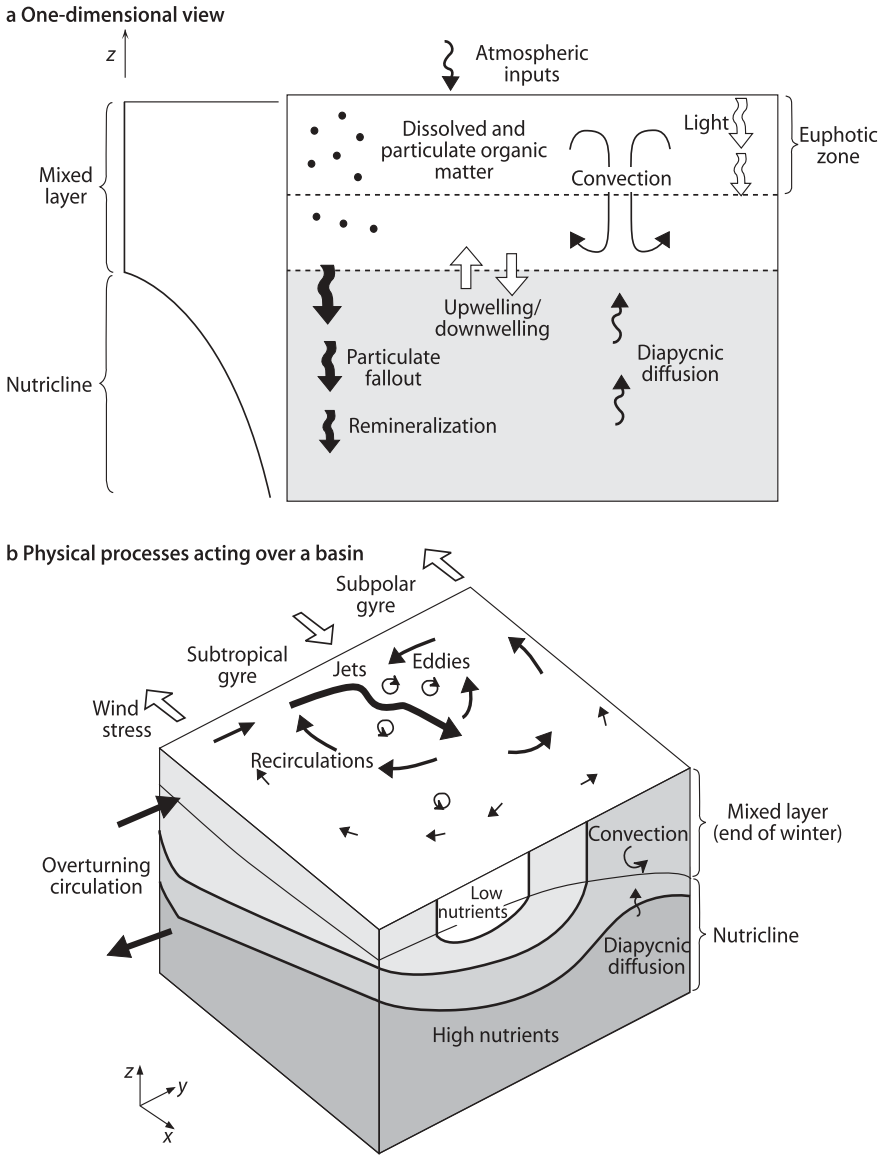

Fig. 2.1.
Schematic figure displaying one- and three-dimensional views of the physical proc esses affecting biological production: **a** In the vertical, there is a phytoplankton growth within the ecosystem, export of organic matter and remineralisation at depth, which is partly maintained through the physical transfer of nutrients within the ocean involving vertical advection, diapycnic diffusion and convection; **b** a more complete view includes the physical transfer of nutrients by the three-dimensional circulation involving contributions from the overturning, gyre, eddy and frontal circulations, as well as involving interactions with spatial variations in convection

2.2 Global Overturning Circulation and Nutrient Transport

2.2.1 Overturning Circulation and Water-Mass Distributions

The overturning circulation transports water masses and nutrients through individual basins and, via the Southern Ocean, around the globe; see reviews by Schmitz (1995) and Zenk (2001). The transport is primarily achieved by narrow boundary currents, jets and recirculating gyres (together with contribution from eddies, particularly over the Southern Ocean). An estimate of the global ocean circulation from Macdonald (1995) is shown in Fig. 2.2, determined from observed sections of temperature, salinity and tracers using an inverse model; also see Macdonald and Wunsch (1996) and Macdonald (1998). This inverse solution emphasises the separate overturning circulations contained within each basin and their connection with the Southern Ocean, as well as basin-scale recirculations. There is a mean northward transport of relatively warm surface waters in the Atlantic Basin (*red arrow* in Fig. 2.2), a transformation to colder, deep waters at high latitudes, and a return southwards transport of cool waters at depth (*blue arrow* in Fig. 2.2). There is a strong eastwards volume flux associated with the Antarctic Circumpolar Current. There are influxes of cold deep waters into the Indian and Pacific Oceans and return flow of warmer water, including a warm-water pathway from the Pacific to Indian Ocean.

This hydrographic solution is more complex than the widely held view of the global circulation as a large overturning cell, often described as the 'conveyor-belt' circulation (Broecker 1991). The distributions of longer-lived oceanic tracers, such as radiocarbon, and the accumulation of nutrients are consistent with the latter view. However, the global hydrographic analyses (e.g. Schmitz 1995) and inverse models (Macdonald and Wunsch 1996; Fig. 2.2) suggest a more complex global circulation, emphasizing separate overturning cells in the Atlantic and Pacific Basins each connecting independently with the Southern Ocean. This more complex circulation is also found to be consistent with the nutrient distributions in inverse models (Ganachaud and Wunsch 2002).

Meridional nutrient sections broadly reflect the classic water-mass distributions over the globe (Fig. 2.3), but have elevated vertical and basin contrasts compared with other characteristics, such as temperature. Water masses are formed within the mixed layer and then transferred into the ocean interior involving a combination of subduction, deep convection and mixing at overflows. In the North Atlantic, surface waters are nutrient depleted and are transformed to intermediate and deep waters at high latitudes. North Atlantic Deep Water (NADW) is formed through a combination of overflow waters, spreads southwards (*green* in Fig. 2.3a) and gradually increases in nutrient concentration by the accumulation of remineralised nutrients from organic fallout. In the Southern Ocean, the deep waters circulate around the globe acquiring high nutrient concentrations through exchanges with Pacific waters and further accumulation of remineralised sinking particulate matter. These nutrient-rich waters of the Southern Ocean partly return into the Atlantic through the northwards flux of Antarctic Intermediate Water (AAIW) and Antarctic Bottom waters (AABW) (*orange* in Fig. 2.3a).

In contrast, the deep and bottom waters of the Pacific are not ventilated locally. Instead the water masses are advected into the Pacific from the Southern Ocean (Fig. 2.3b) where they have acquired characteristically high concentrations in silica. The deep waters spread northwards and continue to accumulate nutrients from sinking particu-

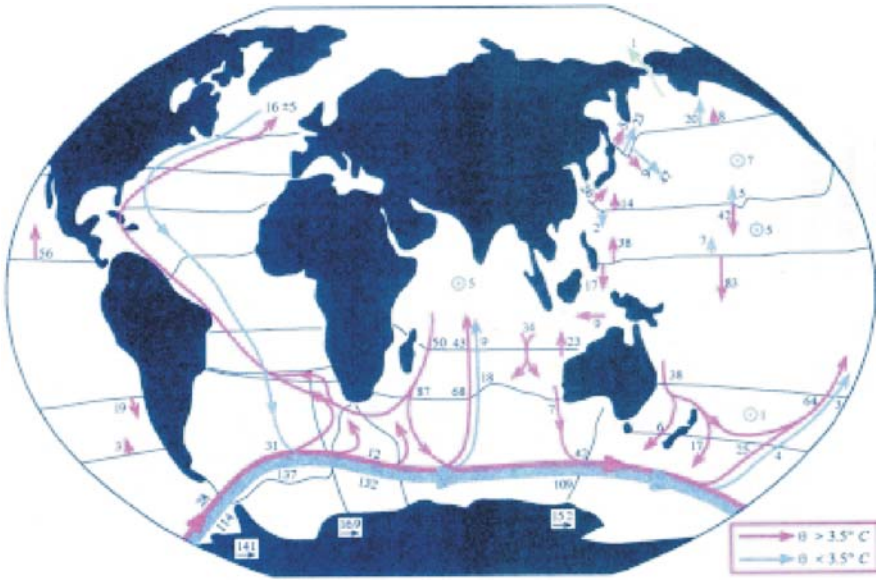

Fig. 2.2.
Global inverse solution for the ocean circulation from Macdonald (1995): *red* and *blue lines* depict the volume transport (Sverdrup; 1 Sv = 10^6 m^3 s^{-1}) associated with fluid warmer or cooler than 3.5 °C respectively. The overturning cell over the Atlantic is revealed with 16 Sv of cold water exported from the North Atlantic, as well as strong zonal transports over the Southern Ocean

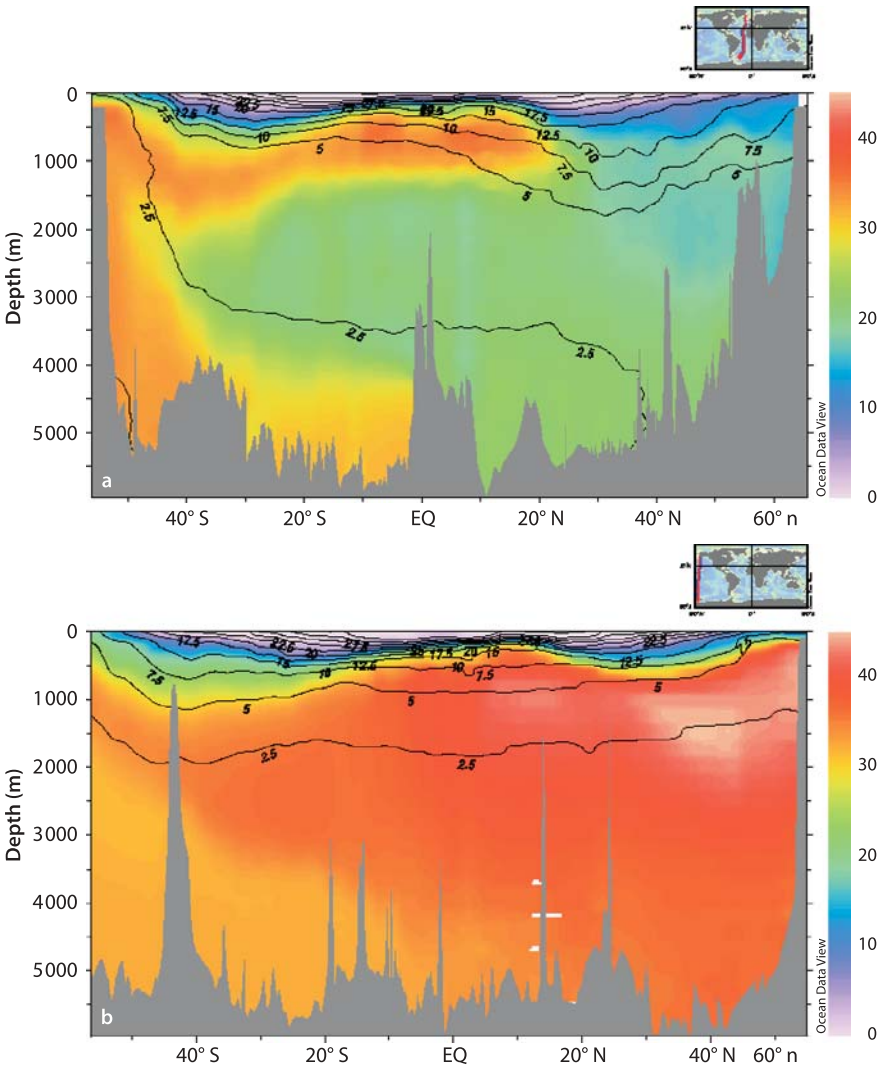

Fig. 2.3.
Meridional WOCE sections of nitrate (*colour shading* in μmol kg^{-1}) and potential temperature (*contours* in °C) for **a** Atlantic (A16) and **b** Pacific (P15). In the Atlantic, there are signals of a southwards spreading of North Atlantic Deep Water (*green*), as well as northwards spreading of Antarctic Intermediate Water and Antarctic Bottom Water (*upper and lower orange plumes*). In the Pacific, there is a northwards influx of bottom and deep water from the Southern Ocean, which is probably returned southwards at mid-depth

lates. There is also a northwards spreading of AAIW in the Pacific (Hanawa and Talley 2001); but this signal is not pronounced in Fig. 2.3b due to the high background nutrient concentrations. The silica distributions suggest that the deep and bottom waters in the Pacific are eventually returned southwards at mid-depths to the Southern Ocean, rather than transformed locally into surface waters (Gnanadesikan 1998; Wunsch et al. 1983). The restriction of ventilation to the upper waters of the North Pacific leads to the underlying mid-depth waters having a local maximum in apparent oxygen utilisation and the highest nutrient concentrations over the global ocean.

2.2.2 Southern Ocean

The Antarctic Circumpolar Current (ACC) is the dominant feature of the Southern Oceans, circumnavigating the globe, and connecting the separate ocean basins; see Rintoul et al. (2001) for a comprehensive review. The surface nitrate distribution across the Southern Ocean is characterised by high concentrations to the south of the Polar Front and lower concentrations to the north[(2)]. The meridional transport of water masses across the Southern Ocean varies with depth: upper waters spread northwards including subducted AAIW, while the underlying NADW spreads southwards and AABW spreads northwards along the bottom (Fig. 2.3 and 2.4). These meridional transfers are crucial in redistributing nutrients around the globe and returning nutrients from deep waters to intermediate and surface waters.

2.2.2.1 *Dynamics of the Meridional Transport*

The meridional transport of nutrients and other tracers is described in terms of an idealised, double meridional cell across the Southern Ocean (Fig. 2.4), although the important transfers also involve zonal and meridional excursions that are often linked to topography. The

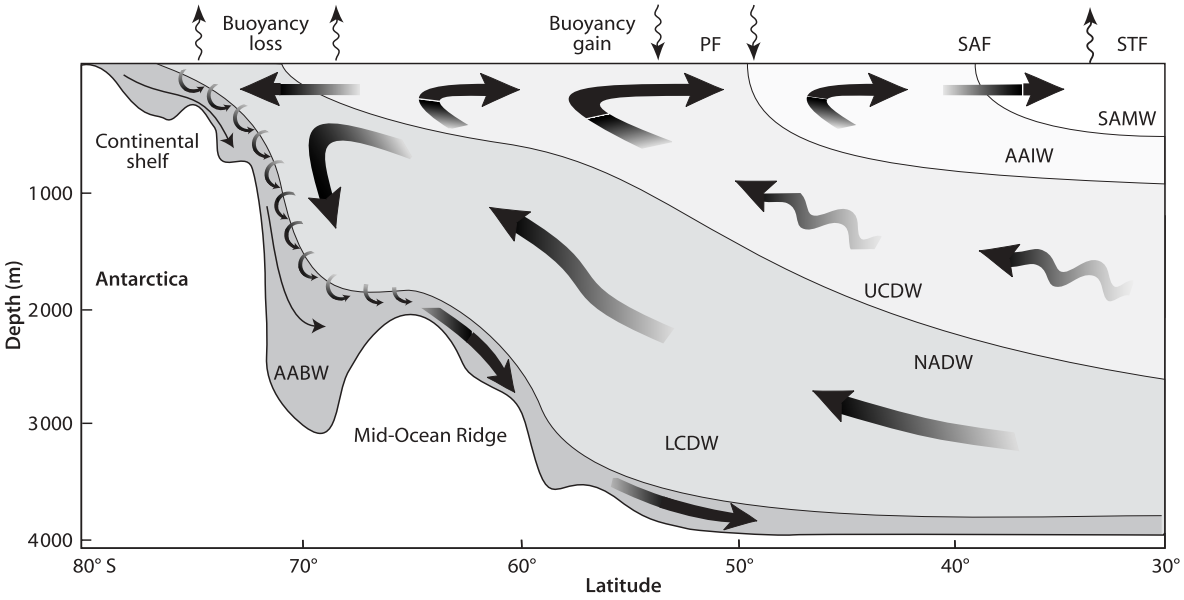

Fig. 2.4. Schematic figure of the two-cell meridional overturning in the Southern Ocean. The upper cell is primarily formed by northwards Ekman transport and gyre transport of surface and Antarctic Intermediate Water (*AAIW*). The lower cell is primarily driven by dense water formation near the Antarctic continent with a northwards transport of Antarctic Bottom Water (*AABW*). Both cells are fed by the southwards transport of Circumpolar and North Atlantic Deep Waters (*NADW*), which is partly achieved by an eddy transport. The Polar Front is denoted by *PF* (reproduced from Speer et al. (2000))

meridional transfer involves different dynamical balances throughout the water column:

i In the upper cell, the westerly wind drives a northwards Ekman transport across the ACC (Toggweiler and Samuels 1995). Nutrient-rich and fresh AAIW is formed north of the Polar Front and probably involves a freshening and cooling of Subantarctic Mode Water in the SW Pacific (McCartney 1977). AAIW is subducted and spreads northwards probably via the gyre circulation between continental barriers.
ii In the lower cell, AABW spreads northwards along the bottom through a geostrophic flow supported by pressure contrasts across topographic ridges.
iii The return flow of the upper and lower cells is associated with the southwards spreading of NADW. This NADW spreading is fed from the northern hemisphere, rather than by a local 'Deacon' cell with diabatic transfer across the thermocline (as misleadingly implied by averaging velocities at fixed points and depths). The physical balance controlling this southwards return flow is still an open question. General circulation models suggest that the southwards spreading is achieved through an adiabatic eddy transport involving contributions from standing and transient eddies (Döös and Webb 1994; Danabasoglu et al. 1994; McIntosh and McDougall 1996)[3].
iv Finally, NADW upwells south of the Polar Front and is converted to lighter surface waters through surface buoyancy gain, as well as converted to denser AABW through surface buoyancy loss (Speer et al. 2000).

2.2.2.2 *Interplay of Transport and Biology*

Nutrient distributions across the Southern Ocean, as elsewhere, are controlled by the competition between biological production and transport. Biological production is always acting to increase the nutrient concentrations in deep waters, whereas transport processes act to decrease the vertical contrast. This competition is illustrated here through idealised integrations of a global biogeochemical model. The model transport includes Ekman and parameterised eddy-induced transport contributions (as depicted later in Fig. 2.21). In the surface ocean, inorganic nutrients are converted to organic nutrients based on a prescribed lifetime. The organic nutrients are exported as sinking particles, falling rapidly relative to the vertical circulation, and are remineralised at depth based on an e-folding depth scale.

Export and remineralisation act to reduce nutrient concentrations in the surface and increase them in the thermocline, enhancing the vertical gradient. In upwelling regions, the nutrient transport acts to further enhance this gradient by supplying nutrients from below, whereas it is weakened in downwelling regions. When the efficiency of biological export is weak relative to the advective transport, the gradients in nutrients become eroded and surface nutrient concentrations become high (Fig. 2.5, *top panel*). When biological export is strong relative to transport, the gradients become strong – both vertically and horizontally – and surface nutrient concentrations become very low (Fig. 2.5, *bot-*

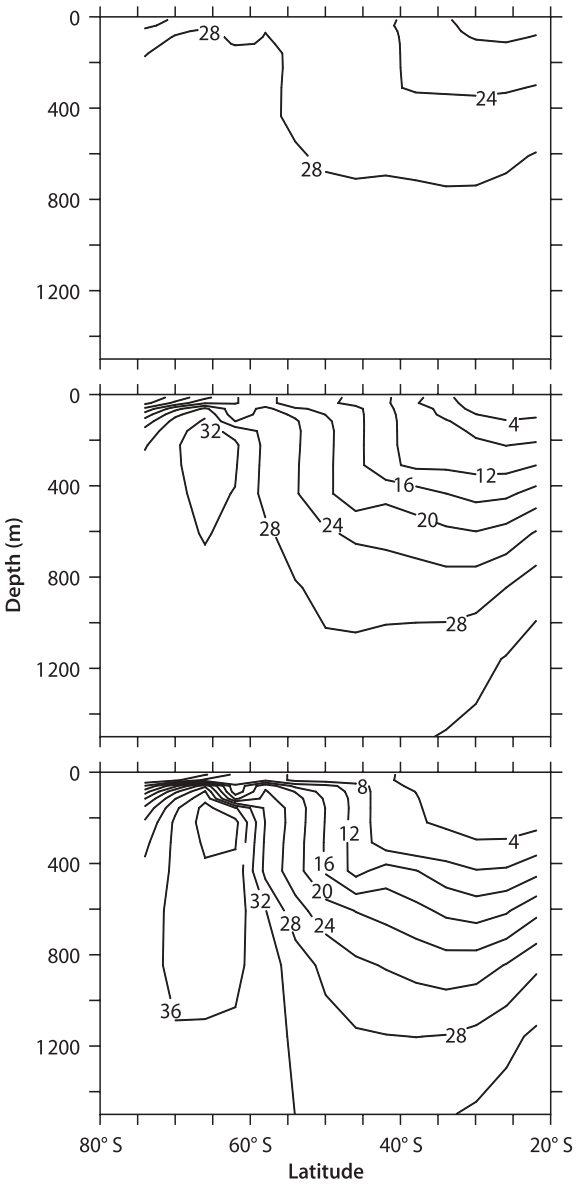

Fig. 2.5. Idealised nutrient experiments over the Southern Ocean from a coarse resolution ocean circulation and biogeochemical model, which illustrate the roles of transport and biological processes in setting nutrient distributions and export production. Inorganic nutrients are converted into organic nutrients within the surface, euphotic zone (modelled very simply as a specified lifetime in the euphotic zone). The organic nutrients are exported as rapidly sinking, particulate fallout and remineralised to inorganic nutrients at depth (here with an e-folding length scale of 300 m). Inorganic nutrient distributions are controlled by the relative magnitude of the nutrient lifetime in the euphotic zone and the time for fluid to be transported meridionally across domain in the surface waters. In the transport-dominated regime, where the biological export timescale is long relative to the transit time (10 years, *upper panel*), nutrient gradients in the horizontal and vertical are relatively weak and export production is low. For a biologically dominated regime where the export timescale is relatively short (3 months, *lower panel*), there are strong horizontal gradients of nutrients below the euphotic zone and high rates of export production. The Southern Ocean for the present day probably lies in an intermediate regime (*middle panel*) where physical transport and biological influences are comparable

tom panel). The modern Southern Ocean appears to fall in an intermediate regime where the biological and physical influences are comparable (Fig. 2.5, *middle panel*); roughly half the nutrients are exported from the euphotic zone as organic matter and the rest are subducted as inorganic nutrients.

2.2.3 Nutrient Supply to the Northern Basins

The basin contrast in overturning circulation suggests significant differences in nutrient supply with implications for biological production. In the North Atlantic, the overturning might be expected to lead to a net flux of nutrients out of the basin with an inflow of surface, nutrient-depleted waters and an outflow of deep, nutrient-enriched waters. Hence, both the zonally-averaged overturning circulation and the downward biological transfer are likely to *inhibit* the nutrient supply to the euphotic zone and reduce biological production. The converse occurs over the Pacific and Indian Oceans, where the overturning circulation is expected to enhance biological production through the inflow of nutrient-rich waters at depth.

2.2.3.1 *Nutrient Transport over the North Atlantic*

This overturning view of the global transport of nutrients overlooks the regional-scale contributions of many physical processes. For example, Fig. 2.6 shows the zonally-averaged fluxes of nitrate at 24° N and 36° N in the Atlantic estimated from hydrographic data by Rintoul and Wunsch (1991). Analysis of these sections revealed a northwards flux of nitrate in the upper part of the water column associated with the Gulf Stream, also highlighted by Pelegri and Csanady (1991), countered by a southward flux in the deeper waters associated with the NADW. In this particular inversion, the nitrate flux is southward across the basin at 24° N and northwards at 36° N, reaching -8 ± 39 kmol N s^{-1} and 119 ± 35 kmol N s^{-1} respectively. This northwards nitrate flux at 36° N is contrary to the southward flux expected from a simple overturning in the Atlantic. The northwards nitrate flux is instead due to the contribution from the horizontal gyre transport (the product of zonal deviations in nitrate concentration and volume flux) dominating over an opposing contribution from the overturning cell.

However, while the contribution of the horizontal circulation is very important, it is not yet clear whether it necessarily dominates. A more recent global inversion by Ganachaud and Wunsch (2002) shows a net southwards nitrate flux over the North Atlantic, although they were unable to include reliable data along 36° N and directly compare with the diagnostics of Rintoul and Wunsch (1991). The relative abundance of nitrate to phosphate, however, suggests that the subtropical North At-

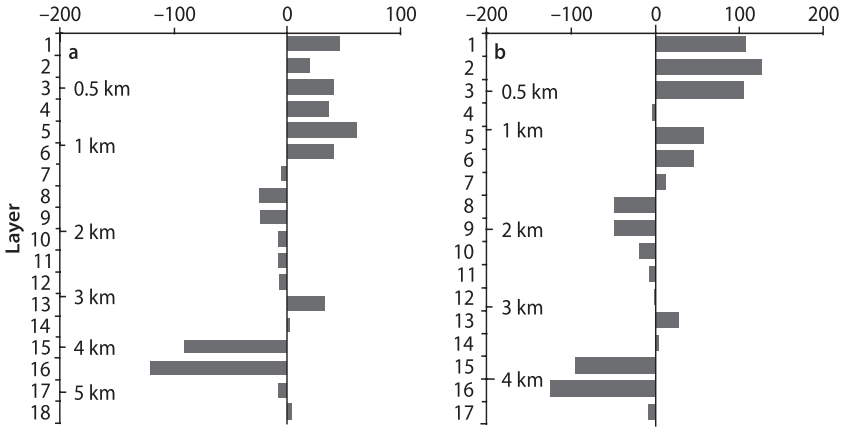

Fig. 2.6.
Zonally-averaged fluxes of nitrate over model layers (10^3 mol N s^{-1}) for **a** 24° N and **b** 36° N in the N. Atlantic from an inverse solution of Rintoul and Wunsch (1991). The net transport of nitrate across 24° N is −8 ±39 kmol N s^{-1}, which is indistin-guishable from zero, while there is net northwards transport of nitrate across 36° N of 119 ±35 kmol N s^{-1}. Each layer corresponds approximately to a neutral surface with layer 1 at the surface and layer 18 at the seafloor; the typical depths are included (redrawn from Deep-Sea Res. 1, 38, Rintoul SR and Wunsch C, Mass, heat, and oxygen budgets in the North Atlantic Ocean, S355–S377, Copyright (1991), with permission from Elsevier Science)

lantic may be a source of new nutrients through nitrogen fixation (Michaels et al. 1996; Gruber and Sarmiento 1997), which would be qualitatively consistent with a net southwards nitrate flux out of the North Atlantic.

In summary, the nutrient transports by the vertical and horizontal large-scale circulation are opposing and both significant over the North Atlantic. The role of transport as a net source or sink of nitrogen to the basin has not yet been decisively identified. An uncertainty arising from inverse models is whether the inversion is chosen to apply globally or locally, which either leads to global constraints being satisfied or particular hydrographic sections being simulated. In addition, there is the potentially important omission of the transport of organic nitrogen, as raised by Rintoul and Wunsch (1991).

2.2.4 Summary

The overturning circulation is important in determining the global distribution of nutrients in the ocean and in supplying nutrients to the upper ocean where biological productivity occurs. On seasonal to interannual timescales, however, biological productivity is more sensitive to the basin-scale gyre circulations, which control regional upwelling and downwelling patterns close to the surface, and to convective activity, which controls the transfer of nutrients through the seasonal-boundary layer to the euphotic zone. We now focus in more detail on the influence of these physical processes including convection, the gyre circulation, and finer-scale eddy and frontal circulations.

2.3 Convection

Surface convection occurs throughout the ocean in response to a surface buoyancy loss or wind stirring; see the review by Marshall and Schott (1999). The combination of solar irradiance and atmospheric forcing induces characteristic diurnal and seasonal cycles in the mixed-layer thickness. Convective changes can alter biological production through the nutrient and trace metal supply to the euphotic zone, change the light experienced by phytoplankton, as well as impact on grazers and community structure. Here, we focus on the seasonal changes in nutrient supply and light received by phytoplankton.

2.3.1 Vertical Transfer of Nutrients

Convection increases the surface nutrient concentrations whenever the mixed layer thickens and nutrients are entrained from the underlying thermocline (Fig. 2.7a). The maximum thickness of the mixed layer usually occurs at the end of winter (defined by when the surface buoyancy loss to the atmosphere ceases) and denotes the extent of the seasonal boundary layer.

2.3.1.1 *North Atlantic Example*

Over the North Atlantic, the surface buoyancy loss at high latitudes leads to a pronounced thickening of the mixed layer at the end of winter (Fig. 2.7b). Convection redistributes nutrients vertically within this layer every year; a climatological estimate of the annual convective supply of nitrate to the euphotic zone is shown in Fig. 2.7c (Williams et al. 2000). The convective supply broadly increases polewards as the winter mixed-layer thickens and ranges from 0.05 to 1.4 mol N m^{-2} yr^{-1} over the basin. There is a similar magnitude of the convective flux diagnosed from in situ observations at Bermuda of 0.1 mol N m^{-2} yr^{-1} (Michaels et al. 1994). In addition, there are interannual variations in the mixed-layer thickness, surface nitrate and chlorophyll cycles, as discussed later in relation to Fig. 2.24 for the Bermuda Time-Series site.

2.3.2 Biophysical Interactions and Convection

The supply of macro-nutrients to the euphotic zone is only one factor in constraining the levels of biological

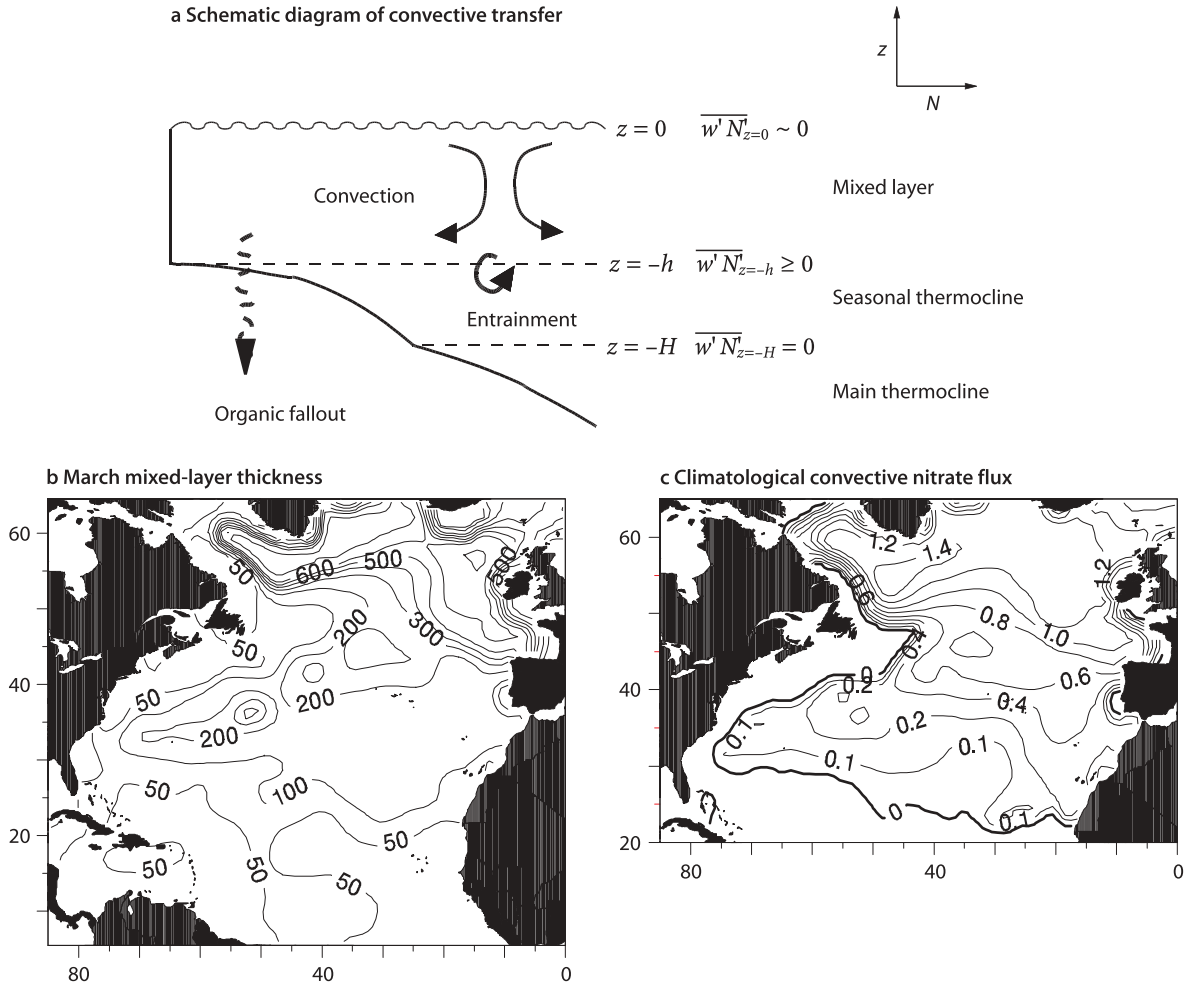

Fig. 2.7. a Schematic figure for the convective boundary layer denoting the variations in the vertical turbulent nutrient flux, $\overline{w'N'}$, where w is a vertical velocity and N is a nutrient concentration (a *prime* denotes a turbulent deviation and an *overbar* represents a time-average over many turbulent events). Climatological estimates of **b** end of winter mixed-layer thickness (m) and **c** convective flux of nitrate (mol N $m^{-2} yr^{-1}$) into the upper 100 m over the North Atlantic. The thickness is diagnosed from climatological density profiles assuming a density increase of 0.125 kg m^{-3} from the surface. The convective flux is diagnosed by combining the seasonal change in mixed-layer thickness with climatological nitrate profiles. For further details, see Williams et al. (2000)

activity, for example, as measured by the amplitude and timing of the annual maximum phytoplankton abundance. A strong spring bloom occurs over the North Atlantic, but not over the North Pacific or Southern Ocean. The lack of a spring bloom and full macro-nutrient drawdown over much of the global ocean has been explained in terms of different hypotheses involving iron and trace metal limitation, light limitation or zooplankton grazing; these competing processes are reviewed by Fasham (1995).

2.3.2.1 *Response of the North Atlantic Bloom*

There are contrasting responses in the phytoplankton growth over the subpolar and subtropical gyres of the North Atlantic; also see Strass and Woods (1991) for a description of how the passage of the bloom leads to a subsurface, deep chlorophyll maximum extending over the North Atlantic.

In the subpolar region, the winter mixed layer may be hundreds of metres thick and nutrients may be abundant. Photosynthesis is light limited during winter, so the bloom occurs in spring when the mixed layer shoals sufficiently to allow phytoplankton to remain within the sunlit region and enable net growth (Sverdrup 1953) (Fig. 2.8a, *left panel*). Here, enhanced convective mixing during the bloom period, perhaps due to the passage of storms, leads to a *weakened* bloom through phytoplankton spending less time in the euphotic zone.

In the subtropical gyres, insolation and stratification are both strong, and winter mixed layers may be only 100 m or so thick. The system is nutrient limited and the bloom occurs in winter when the mixed layer deep-

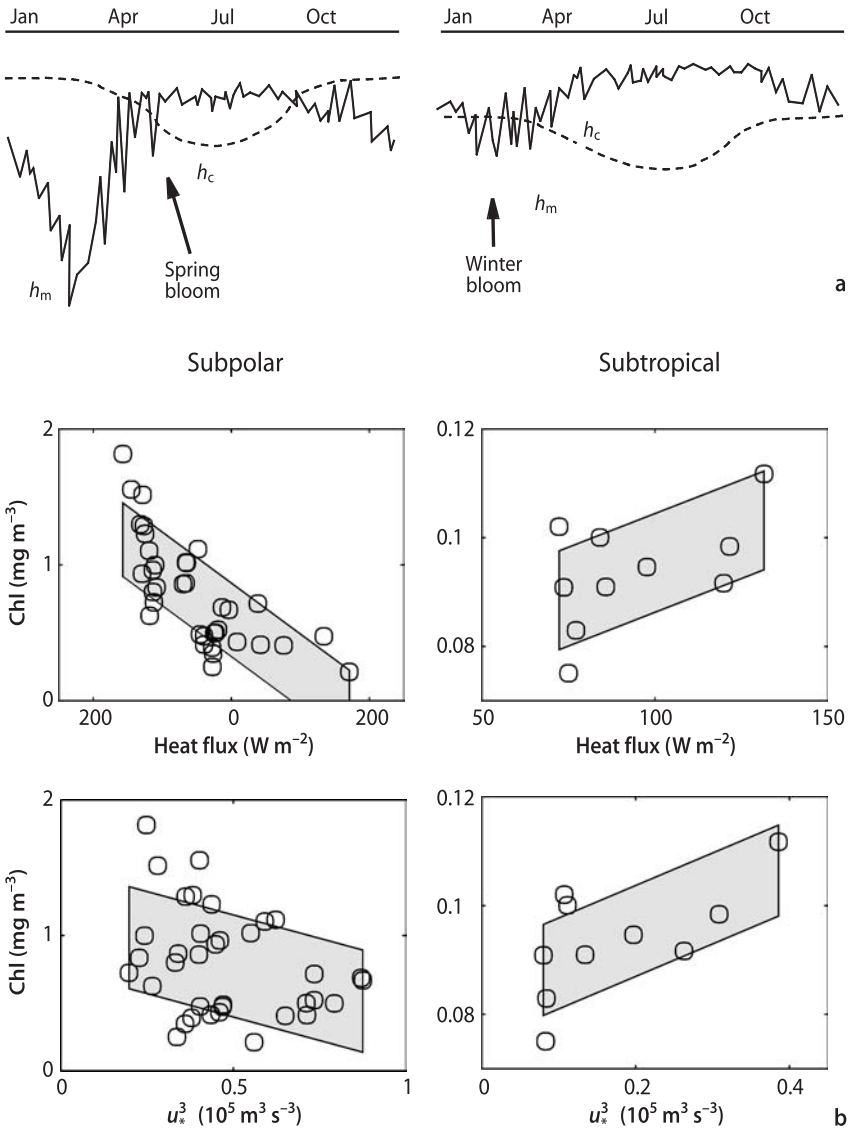

Fig. 2.8.
a Schematic depiction of the annual cycle of mixed-layer thickness (h_m) and critical layer depth (h_c) for subpolar (*left panel*) and subtropical (*right panel*) regimes. The critical depth is the region where photosynthetic production outstrips respiration or grazing (e.g. Townsend et al. 1994) – this depth is typically up to a few 10s of metres in spring. The mixed-layer thickens in winter and shoals in spring. In the light-limited subpolar region (*left panel*) the bloom occurs in spring when phytoplankton are confined within the critical layer. In the subtropics (*right panel*) it occurs when winter convection supplies nutrients. **b** Illustration of the relationship of bloom intensity and physical forcing for 1997 bloom in the N. Atlantic. The figures show remotely observed chlorophyll (SeaWiFS, level 3) vs. heat flux out of the ocean (W m^{-2}) and wind forcing (m^{3}s^{-3}) (Follows and Dutkiewicz 2002); the latter defined by a friction velocity cubed derived from NCEP reanalysed meteorological data. The bloom-period is defined here as the two months bracketing the annual maximum surface chlorophyll at each latitude, and data points represent area averages from 5° square regions. In the subpolar region (*left panel*), the bloom is more intense where greatest heat input favours restratification. In the subtropical region (*right panel*), the bloom is intensified where there is greater surface heat loss and wind mixing, consistent with nutrient limitation. The *shading* denotes one standard deviation either side of a linear least squares fit (redrawn from Deep-Sea Res. II 49, Follows MJ and Dutkiewicz S, Meteorological modulation of the North Atlantic spring bloom, 321–344, Copyright (2002), with permission from Elsevier Science)

ening provides new nutrients (Menzel and Ryther 1961) (Fig. 2.8a, *right panel*). Here, enhanced convection during the bloom period leads to a *strengthened* bloom through the increase in nutrient supply.

These regimes and responses can be identified in the North Atlantic ocean from remote ocean colour observations and meteorological data as illustrated in Fig. 2.8b (Follows and Dutkiewicz 2002; Dutkiewicz et al. 2001). The subtropical and subpolar regimes exhibit opposing relationships to regional changes in surface heat flux out of the ocean and wind mixing. In the subpolar region, the bloom occurs during periods of restratification (Fig. 2.8b, *left panel*) when the heat flux is into the ocean (marked as negative values). The strength of the bloom is inversely proportional to the strength of wind mixing. The opposite is true in the subtropical region where there is a positive correlation between chlorophyll concentration and the heat flux out of the ocean, as well as with the strength of wind mixing (Fig. 2.8b, *right panel*). These responses are consistent with the phytoplankton growth being initially limited by light over the subpolar gyre and instead by nutrients over the subtropical gyre. The broad classification of subtropical and subpolar regimes, along with other significant processes, such as zooplankton grazing, ecological variability and mesoscale motions leads to a significant spread in the data (as marked by the *shaded regions* in Fig. 2.8b indicating one standard deviation either side of a linear least squares fit).

2.3.2.2 *Role of Convective Plumes*

Convection involves an overturning of dense water in narrow plumes with horizontal scales of a few kilometres (Marshall and Schott 1999). Convection is traditionally represented in models by turbulent mixing in the

vertical, rather than an advective transfer. In many situations, the integrated effect of many convective plumes is equivalent to large-scale turbulent mixing. It is possible, however, that the biogeochemical processes might be sensitive to the vertical velocities associated with convective plumes. The localised sinking in a plume is accompanied by larger-scale upwelling, such that the overall downwards mass flux is close to zero. This compensating upwelling can prevent the sinking of phytoplankton, zooplankton and the fallout of organic matter during winter (Backhaus et al. 1999). *If* organic particles are produced at a constant rate over the winter period, then organic fallout to the deep ocean should locally peak when convection ceases following a surface buoyancy input. There may then be a subsequent burst in 'new' organic fallout associated with any subsequent spring bloom.

The restratification of convective plumes is also significantly altered by lateral buoyancy transfers by mesoscale eddies (Marshall and Schott 1999). Consequently, the emergence of the spring bloom and its spatial character and intensity in region of deep convection can partly depend on the baroclinic eddy scales (Lévy et al. 1998; see later discussion).

2.3.3 Limited Role of Convection

Convection provides significant nutrient fluxes to the euphotic zone, but by itself only has a limited role in maintaining biological production over timescales of several years or more. Convection redistributes nutrients within the seasonal boundary layer with the convective flux of nutrients vanishing at the base of the winter mixed layer. Hence, if there is fallout of organic matter out of the base of the winter mixed layer, the nutrient concentration over the seasonal boundary layer will gradually decrease in time unless there is another source of nutrients. This result is illustrated in the following derivation.

Consider the evolution of a nutrient, N, representing the sum of inorganic and dissolved organic forms, which may be written as

$$\frac{\partial N}{\partial t} + \nabla.(uN) + \frac{\partial}{\partial z}\overline{w'N'} = \frac{\partial F}{\partial z} \tag{2.1}$$

The supply of N is controlled by the divergence of the advective fluxes, uN, and the vertical divergence of the turbulent fluxes, $\overline{w'N'}$, within the mixed layer (representing convective mixing). Here u is the three-dimensional velocity vector and w' is the turbulent vertical velocity where a prime represents a turbulent event in the mixed layer and an overline represents a time-average of these turbulent events. F represents the vertical sinking flux of particulate organic matter, and $\partial F/\partial z$ represents the net rate of biological consumption or regeneration of N in terms of a vertical flux divergence.

On seasonal timescales, the evolution of N over a surface layer (representing either a mixed layer or the euphotic zone) is largely controlled by a one-dimensional balance. Integrating Eq. 2.1 over this layer of thickness h (Fig. 2.7a), and neglecting advective and surface sources leads to

$$h\frac{\partial N}{\partial t} \approx \overline{w'N'}_{z=-h} - F(-h) \tag{2.2}$$

where N in the surface layer increases in concentration through convective mixing and entrainment in winter and decreases in summer through biological consumption and export; $\overline{w'N'}_{z=-h}$ represents a turbulent flux of nutrients into the surface layer from the entrainment of nutrient-rich, thermocline fluid and $F(-h)$ represents the export flux of organic matter out of the surface layer.

However, if this nutrient balance (Eq. 2.1) is instead integrated over the seasonal boundary layer (defined by the maximum thickness, H, of the winter mixed layer), then the entrainment flux vanishes, $\overline{w'N'}_{z=-h} \approx 0$, below this level (Fig. 2.7a). *If* advective and surface sources of nutrients are again neglected, as well as diffusion within the thermocline, then

$$\frac{\partial}{\partial t}\int_{-H}^{0} N dz \approx -F(-H) \tag{2.3}$$

This balance implies that the nutrients within the surface boundary layer will eventually be exhausted through biological export into the main thermocline, since the right-hand side of Eq. 2.3 is negative. Consequently, a flux of nutrients into the seasonal boundary layer is required in order to offset this loss and maintain nutrient concentrations. Wind-driven gyre and eddy transfer mechanisms may account, at least in part, for this source, and are discussed later.

2.3.4 Summary

Convection provides a nutrient flux into the euphotic zone, as well as altering the light phytoplankton receive by modifying how much time they spend in the euphotic zone. Seasonal or interannual changes in convection have contrasting effects on biological production according to whether phytoplankton growth is limited by the availability of nutrients or trace-metals, or by the light received. Convection only redistributes nutrients within the seasonal boundary layer. Consequently, other processes, such as advective transport, must provide a nutrient source to the seasonal boundary layer offsetting the loss from export of organic matter organic fallout into the underlying thermocline.

2.4 Wind-Driven Circulations: Gyres and Boundary Currents

2.4.1 Wind-Induced Upwelling and Gyre Circulations

The atmospheric winds induces a horizontal (Ekman) volume flux over the surface (Ekman) layer of the upper ocean, directed to the right of the wind stress in the northern hemisphere and to the left in the southern hemisphere[4]. A horizontal divergence of this volume flux in turn drives upwelling into the surface Ekman layer and, conversely, a horizontal convergence drives downwelling.

2.4.1.1 *Tropical and Coastal Upwelling*

Over the tropics, the surface Trade winds are generally directed westwards and equatorwards (as part of the atmospheric Hadley circulation). Accordingly, this wind pattern drives a polewards Ekman volume flux on either side of the equator (Fig. 2.9a) and an off-shore Ekman flux along the eastern boundary of an ocean basin. Consequently, the divergence of this horizontal Ekman volume flux drives a band of upwelling along the equator, which extends along the eastern boundary.

This equatorial and coastal upwelling supplies macronutrients to the euphotic zone elevating local productivity; see later Fig. 2.23 (*lower panel*) for an example of elevated chlorophyll in the equatorial Pacific due to equatorial and coastal upwelling. Since coastal upwelling is driven by the local winds, the nutrient supply is modulated on atmospheric synoptic timescales. A succession of phytoplankton species follow upwelling events and the frequency of such events can modulate the dominant community structure; see reviews of the physical and biogeochemical aspects of coastal upwelling systems by Smith (1995) and Hutchings et al. (1995) respectively.

2.4.2 Gyre-Scale Circulations

The surface winds drive double-gyre systems over ocean basins (Fig. 2.9a,b). Subpolar gyres are characterised by a cyclonic circulation, upwelling and a raised thermocline. Conversely, subtropical gyres are associated with an anticyclonic circulation, downwelling and a depressed, thicker thermocline. These thermocline changes are reflected in the nutrient distribution with uplifted or depressed nutriclines occurring over the subpolar and subtropical gyres respectively (see Fig. 2.3). In turn, there are generally higher concentrations in remotely-sensed estimates of surface chlorophyll and primary production over the subpolar gyre (Fig. 2.10) (Sathyendranath et al. 1995; Behrenfeld and Falkowski 1997). Higher levels of primary production generally appear to coincide with upwelling regions over the subpolar gyre and along coastal boundaries (Fig. 2.10) (Williams and Follows 1998a; McClain and Firestone 1993).

The subtropical and subpolar gyre circulations are directly connected to each other. For an idealised wind-driven double-gyre, fluid particles follow trajectories making up an idealised 'figure of eight' (Fig. 2.9c):

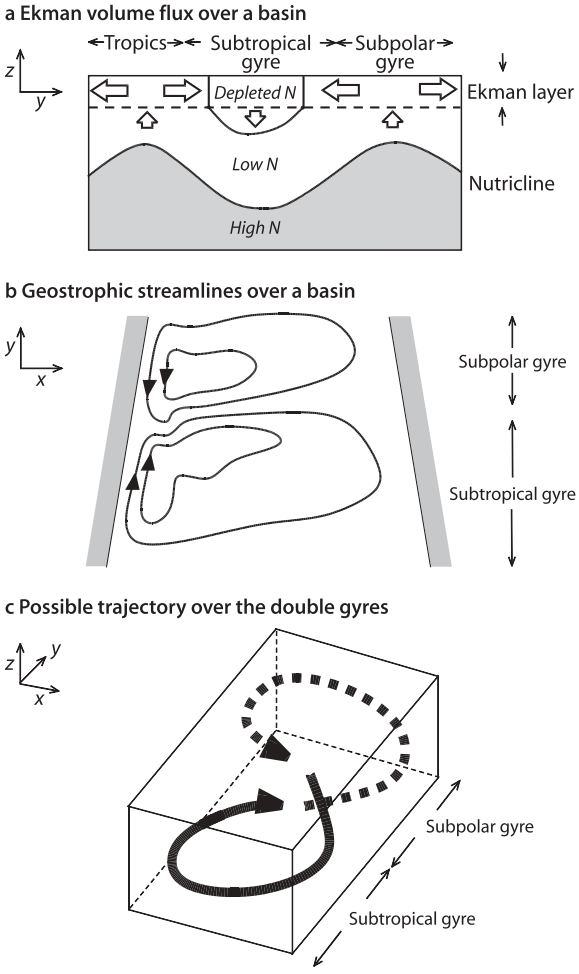

Fig. 2.9. Schematic figure of the gyre circulation within a basin: **a** Ekman volume fluxes along a vertical meridional section, **b** surface view of geostrophic streamlines, and **c** possible trajectory circuiting the double gyre system (*dashed* and *full lines* are within the subpolar or subtropical gyres respectively). Divergence of the horizontal Ekman flux induces upwelling and a raised nutricline in the tropics and subpolar gyre, as well as downwelling and a depressed nutricline in the subpolar gyre. The surface geostrophic flow follows a cyclonic pattern over the subpolar gyre and an anticyclonic pattern over the subtropical gyre. Fluid is exchanged between the gyres through a boundary current transport along the western boundary, as well as through an Ekman and time-varying eddy transport over the entire domain. This idealised gyre picture is also modified through the contribution of the overturning circulation, which can further enhance or oppose the gyre transport of upper waters along the western boundary

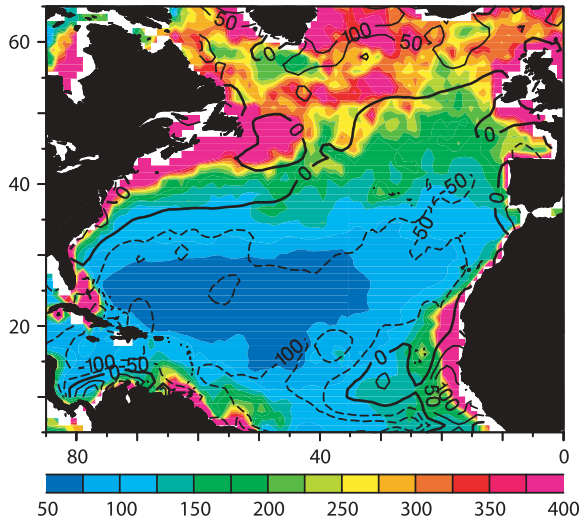

Fig. 2.10. Annual primary productivity (*colour shaded* in mol C $m^{-2} yr^{-1}$) and wind-induced (Ekman) upwelling (*solid contours* in m yr^{-1}). The annual primary productivity is inferred from satellite observations of surface chlorophyll by Sathyendranath et al. (1995) and the upwelling inferred from a wind-stress climatology. The primary productivity shows maximum values in the subpolar gyre and reduced values over the subtropical gyre, broadly following the patterns of gyre-scale upwelling (reproduced from Williams and Follows (1998b))

(*i*) fluid particles upwell and recirculate around the subpolar gyre, (*ii*) transfer into the subtropical gyre through a lateral flux across the inter-gyre boundary, (*iii*) downwell and recirculate around the subtropical gyre, and (*iv*) eventually return to the subpolar gyre via the western boundary current. This interpretation is consistent with simplified models of a subtropical gyre emphasising the balance between a volume influx from the surface Ekman transfer and a volume outflux in the western boundary (Veronis 1973). In a similar manner, nutrients should be transferred between the subtropical and subpolar gyres through the lateral fluxes across the inter-gyre boundaries. This idealised picture is also modified through the overturning circulation acting over the basin.

2.4.3 Subduction and Fluid Transfer into the Seasonal Boundary Layer

The gyre-scale circulation transfers fluid between the mixed layer/seasonal boundary layer and the underlying thermocline (Fig. 2.11a); see Marshall et al. (1993) and a review by Williams (2001). This subduction process helps to determine the properties of the interior ocean. Fluid is preferentially subducted into the main thermocline at the end of winter (due to the seasonal migration of density outcrops) leading to the interior water-mass properties matching those of the mixed layer at the end of winter (Stommel 1979; Williams et al. 1995). Local maxima in the subduction process lead to formation of 'mode' waters, weakly stratified fluid with nearly homogeneous properties, which can spread over relatively large geographic regions (e.g. Hanawa and Talley 2001).

The reverse of the subduction process is important in determining nutrient distributions over the upper ocean, where fluid is transferred from the ocean interior into the seasonal boundary layer. The annual volume flux, or induction flux, into the seasonal boundary layer from the time-mean circulation consists of vertical and horizontal contributions:

$$w_b + u_b.\nabla H \tag{2.4}$$

where w_b and u_b are the vertical velocity and horizontal velocity vector at the base of the seasonal boundary layer with a thickness H and a horizontal gradient ∇H. This contribution of the time-mean circulation can be augmented by a rectified contribution from the time-varying circulation (Marshall 1997). This volume exchange from the time-mean and time-varying circulations determines whether nutrient-rich thermocline waters are advected into the seasonal boundary layer or nutrient-depleted surface waters are subducted into the thermocline. In turn, this advective transfer of nutrients helps to determine whether the surface waters are nutrient rich or poor.

2.4.3.1 *North Atlantic Example*

The induction flux over the North Atlantic is controlled by both the vertical and horizontal transfers between the mixed layer and thermocline (Eq. 2.4). Climatological estimates of the vertical Ekman volume flux and induction flux into the seasonal boundary layer evaluated from climatology are shown in Fig. 2.11b,c; details of the calculation are described in Marshall et al. (1993). The induction flux is evaluated assuming the thickness H is defined by the base of the end of winter mixed layer (Fig. 2.7b).

Over the subpolar gyre, fluid is transferred from the thermocline into the seasonal boundary layer. The induction flux reaches 300 m yr^{-1}, compared to a vertical Ekman flux of only about 50 m yr^{-1} (where the volume fluxes are expressed per unit horizontal area). Therefore, the flux is dominated by the horizontal transfer due to the thickening of the seasonal boundary layer, caused by the surface cooling, along the cyclonic circuit of the gyre. Hence, the nutrient-rich surface waters of the subpolar gyre are sustained through both the horizontal and vertical advective influx from the nutrient-rich thermocline.

Over the subtropical gyre, fluid is subducted from the mixed layer into the thermocline. The induction flux is

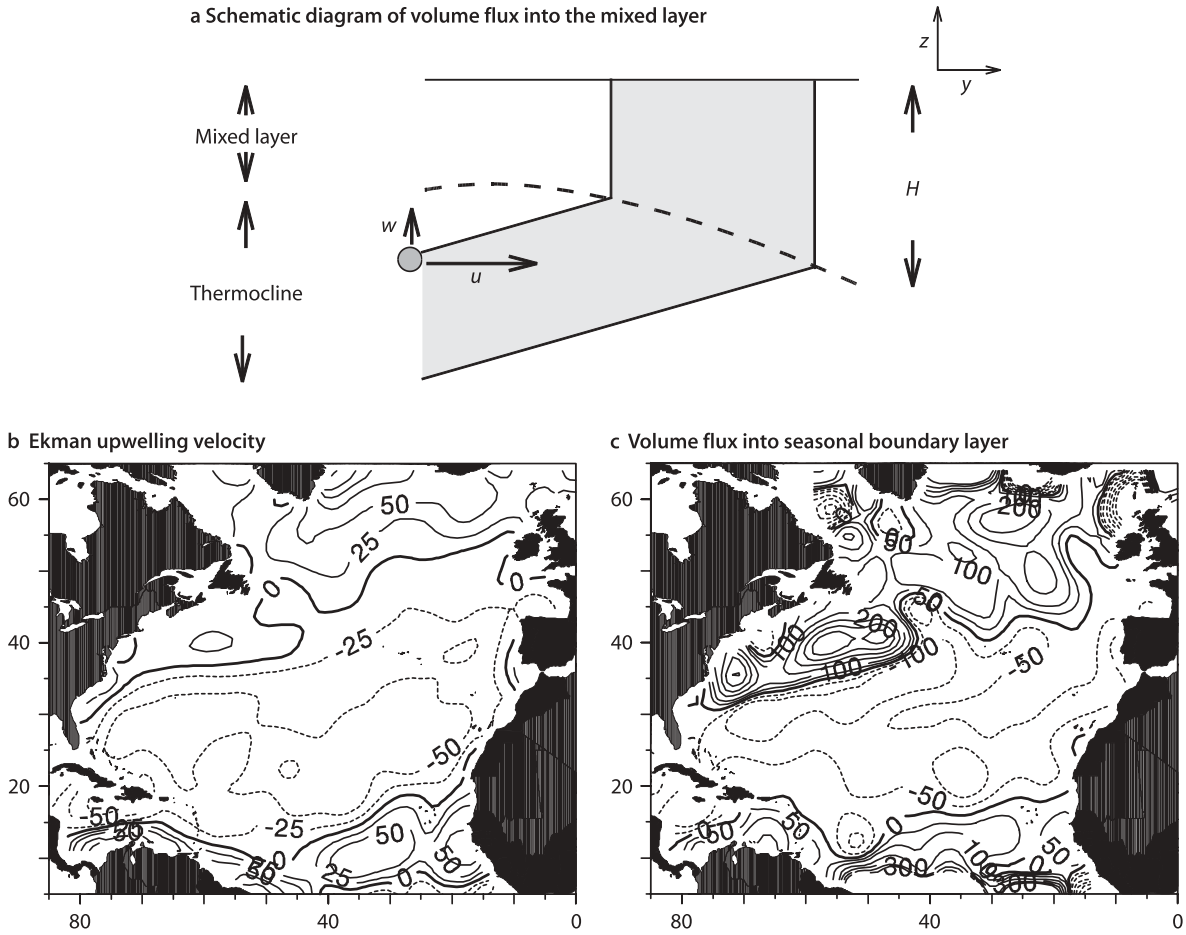

Fig. 2.11. a Schematic figure of the subduction process involving fluid being transferred between the mixed layer and stratified thermocline. A fluid particle is advected by the vertical velocity, w, and horizontal velocity, u. The volume flux into the mixed layer is given by the sum of the vertical and horizontal transfer into the mixed layer: $w + u\nabla H$ where H is the thickness of the mixed layer at the end of winter (or equivalently the extent of the seasonal boundary layer). The lateral transfer is important when the mixed layer thickens polewards, as depicted here. Climatological estimates of **b** Ekman upwelling velocity ($m\,yr^{-1}$) and **c** volume flux into the seasonal boundary layer per unit horizontal area ($m\,yr^{-1}$) for the North Atlantic; see Marshall et al. (1993) for details of the calculation. The volume flux into the seasonal boundary layer in **c** exceeds the contribution from Ekman upwelling **b** due to the lateral transfer

typically –50 m yr^{-1} with similar contributions from the vertical and horizontal transfer. Any surface nutrients are transported into the thermocline by the gyre-scale circulation. The nutrient-rich waters in the thermocline are only likely to reach the euphotic zone over the interior of the subtropical gyre through diapycnic mixing or fine-scale upwelling (discussed later). Instead, the thermocline nutrients are more likely to be transported into the western boundary current and either to recirculate around the subtropical gyre or enter the subpolar gyre.

2.4.4 Oligotrophic Subtropical Gyres

The gyre-scale subduction process leads to surface waters being relatively nutrient rich over the subpolar gyre, and nutrient poor over the subtropical gyre. This different nutrient supply is reflected in patterns of primary production as suggested by remotely-sensed estimates of surface chlorophyll (Fig. 2.10). Much of the primary production is associated with recycling of organic matter, but a fraction is associated with sinking organic particles or dissolved organic matter transported out of the euphotic zone. This fraction is referred to as export production. Estimates of export production over subtropical gyres reach 0.48 ±0.14 mol N $m^{-2}\,yr^{-1}$ in the Sargasso Sea from transient-tracer and oxygen diagnostics (Jenkins 1982, 1988; Jenkins and Goldman 1985), as well as 0.19 mol N $m^{-2}\,yr^{-1}$ near Hawaii from sediment-trap estimates (Emerson et al. 1997).

If these modest levels of export production are representative, then the extensive area of the subtropical gyres means that they might account for half of the global export of organic carbon to the ocean interior (Emerson et al. 1997). Consequently, this level of export

production raises the question of how sufficient nutrients are supplied to the euphotic zone in these oligotrophic waters?

For example, over the Sargasso Sea, the supply of nitrate from the traditionally considered sources only amounts typically to 0.21 mol N $m^{-2}\,yr^{-1}$ (see the review by McGillicuddy et al. 1998); the separate contributions are 0.13 ±0.05 mol N $m^{-2}\,yr^{-1}$ from entrainment (Michaels et al. 1994), 0.05 ±0.01 mol N $m^{-2}\,yr^{-1}$ from diapycnic diffusion (Lewis et al. 1986) and 0.03 mol N $m^{-2}\,yr^{-1}$ from atmospheric deposition (Knap et al. 1986). Accordingly, the shortfall in the nutrient supply over the Sargasso Sea needed to explain the transient-tracer and oxygen based estimates of export production is typically 0.27 mol N $m^{-2}\,yr^{-1}$. Part of this mismatch might be explained by a further source of nitrogen due to nitrogen fixation over the subtropical North Atlantic; this source is implied by a geochemical signal of an increased nitrate / phosphate ratio in the underlying thermocline (Michaels et al. 1996; Gruber and Sarmiento 1997).

In addition, diagnostics of Rintoul and Wunsch (1991) suggest that there is a divergence in the nitrate transport between 24° N and 36° N in the Atlantic (as discussed previously with Fig. 2.6). The additional nutrient flux needed to sustain the levels of export production and the nutrient budget might be provided by the following mechanisms: lateral transfer of nutrients across inter-gyre boundaries, the action of the finer-scale eddy or frontal circulations, or non-advective sources, such as nitrogen fixation or atmospheric deposition of organic nitrogen. The role of the lateral transfer of nutrients is discussed next and later the role of the time-varying circulation.

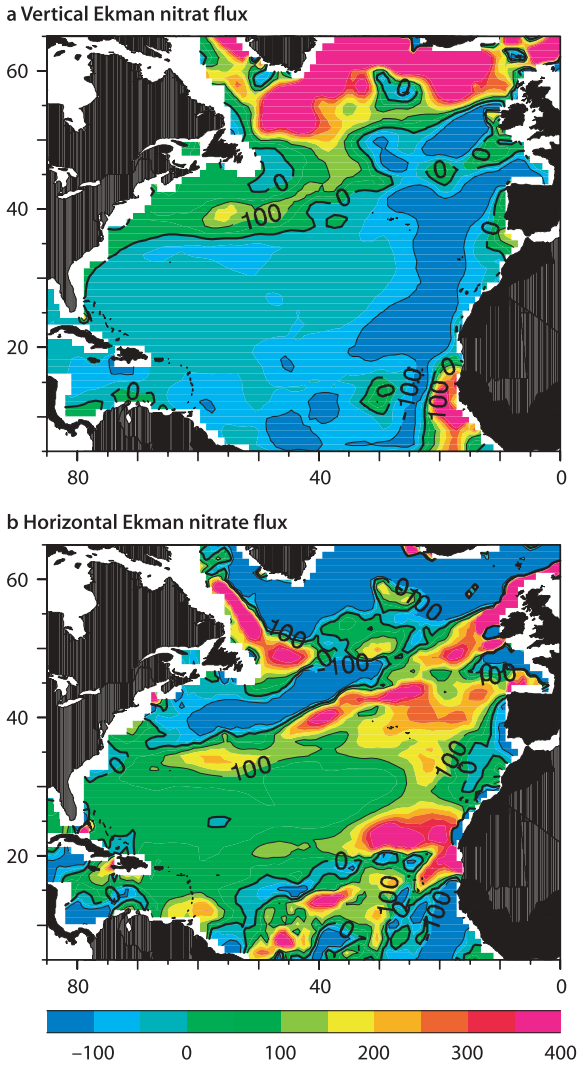

Fig. 2.12. Convergence of Ekman nitrate flux (10^{-3} mol N $m^{-2}\,yr^{-1}$) over the North Atlantic for April for **a** vertical and **b** horizontal components; the diagnostics are based on a climatological analysis (Williams and Follows 1998a). The vertical Ekman transfer provides a nitrate supply to the euphotic zone over the subpolar gyre, while the horizontal Ekman transfer provides a supply over the flanks of the subtropical gyre (reprinted from Deep-Sea Res. I 45, Williams RG and Follows MJ, The Ekman transfer of nutrients and maintenance of new production over the North Atlantic, 461–489, Copyright (1998), with permission from Elsevier Science)

2.4.4.1 *Lateral Transfer of Nitrate*

Downwelling over the subtropical gyre is induced by a convergence of the horizontal Ekman volume flux. These lateral Ekman fluxes likewise transfer nutrients horizontally into the subtropical gyre from the neighbouring nutrient-rich tropics and subpolar gyre (Fig. 2.9a). The convergence of the horizontal Ekman flux of nitrate is significant over the flanks of the subtropical gyre and is comparable to that from the vertical flux over upwelling regions (Fig. 2.12) (as diagnosed from climatology by Williams and Follows 1998a).

The annual Ekman flux of nitrate is dominated by the winter and spring contributions when the surface nitrate concentration is enhanced through entrainment. Over the North Atlantic, the annual convergence of the Ekman horizontal nitrate flux reaches a maximum of 0.1 mol N $m^{-2}\,yr^{-1}$ along the flanks of the subtropical gyre, but decreases rapidly over the gyre interior due to the limited lifetime of nitrate in surface waters.

2.4.4.2 *Lateral Transfer of Organic Nutrients*

Organic and inorganic nutrients can be transported in different directions due to their different spatial distributions and lifetimes in the euphotic zone (Jackson and Williams 1985). For example, total organic nitrogen (TON) is generally surface intensified, whereas nitrate has a higher concentration at depth, and semi-labile TON has a longer lifetime than nitrate in the euphotic zone[(5)]. Rintoul and Wunsch (1991) suggested that organic nitrogen might be transferred into the subtropi-

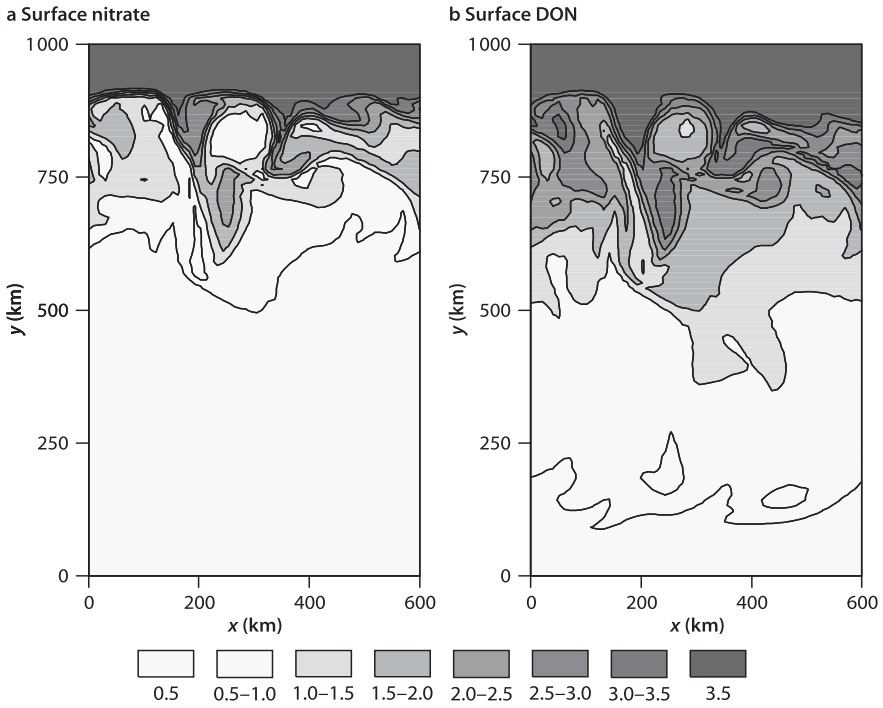

Fig. 2.13.
Modelled distributions of **a** nitrate and **b** dissolved organic nitrogen (DON) (μmol kg^{-1}) in the euphotic zone from an eddy-resolving model for a wind and buoyancy-driven zonal channel. The nutrients are transferred from a northern source equatorwards through a combination of the surface Ekman and eddy circulations. The nitrate and DON are chosen to have lifetimes of 3 and 6 months respectively. Consequently, DON penetrates further equatorwards than nitrate and helps to enhance export production within the interior of the domain (reproduced from Lee and Williams (2000))

cal gyre, offsetting the loss of nitrate and maintaining the total nitrogen budget. Indirect support is provided by observations suggesting that more organic carbon is consumed by respiration in the centre of subtropical gyres, than produced by photosynthesis (Duarte and Agusti 1998). The necessary organic carbon might be laterally transferred into the subtropical gyre along with organic nutrients.

Abell et al. (2000) observe that there is a meridional gradient in surface total organic phosphorus (TOP) over the North Pacific subtropical gyre while there is no significant gradient in TON. These signals are consistent with the hypothesis that any production in the subtropical gyre is sustained by a combination of nitrogen fixation providing the required nitrogen and perhaps a lateral influx of TOP providing the required phosphorus. The organic phosphorus might be brought into the subtropical gyre through a combination of the Ekman and eddy transfer across the intergyre boundaries. This response is illustrated in an eddy-resolving model experiment shown in Fig. 2.13 (Lee and Williams 2000): dissolved inorganic and organic nutrients are released along a northern boundary and are transferred southwards through the Ekman and eddy circulations. The dissolved organic nutrient penetrates further from the source than for inorganic nutrient due to its longer lifetime in the euphotic zone.

Closing the nitrogen and phosphorus budgets requires a systematic set of hydrographic sections including the measurement of organic nutrients. In our view, the lateral transfer of organic phosphorus is likely to be important in closing the budget, but it is unclear whether a lateral transfer of organic nitrogen is needed given the potential role of nitrogen fixation at least over the North Atlantic. In explaining how export production is maintained over subtropical gyres, there is an important additional contribution from time-varying currents (discussed later in relation to Fig. 2.17 and 2.22).

2.4.5 Western Boundary Transport of Nutrients

Western boundary currents are crucial in transporting water masses over ocean basins and providing 'nutrient streams' passing from the subtropical gyre to the subpolar gyre in the upper ocean (as depicted in Fig. 2.9c).

2.4.5.1 *Gulf Stream Example*

Hydrographic sections reveal subsurface, enhanced nutrient fluxes coinciding with the core of the Gulf Stream (Pelegri and Csanady 1991; Pelegri et al. 1996); centred along $\sigma_t = 26.8$ surface at typically 500 m depth, see Fig. 2.14. The nitrate flux associated with the Gulf Stream (defined by the product of the nitrate concentration and the geostrophic velocity normal to the section) increases by a factor of 3 from Florida Strait (24° N) to the mid-Atlantic Bight (36° N) where it reaches 860 kmol N s^{-1}, and then decreases downstream. The increase in nitrate transport along the Gulf Stream can be attributed to the recirculating, nutrient-enriched thermocline waters of the subtropical gyre joining the boundary current. The nitrate flux at the mid-Atlantic Bight partly passes into

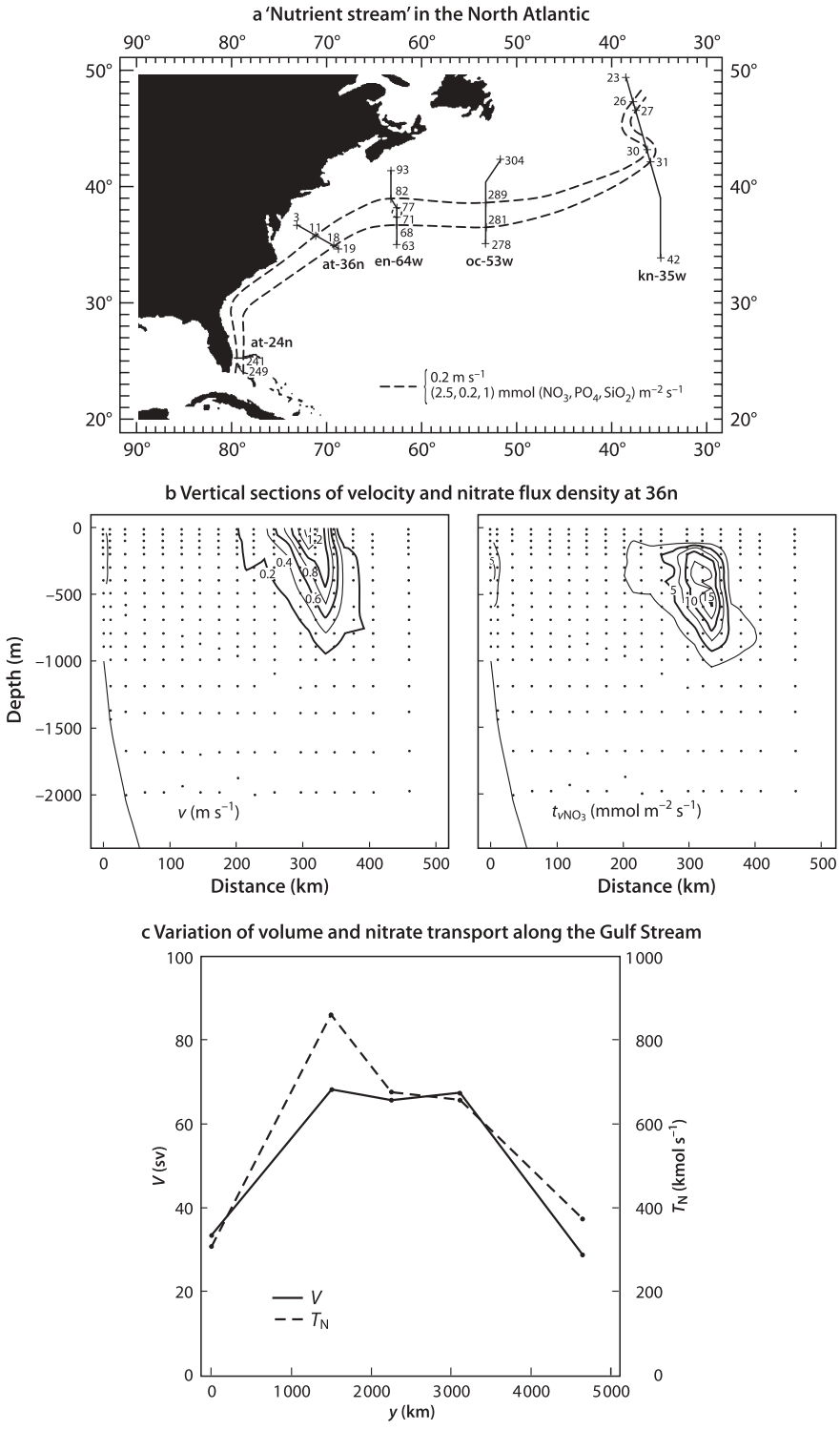

Fig. 2.14.
Diagnostics of how the Gulf Stream acts as a 'Nutrient Stream': **a** *dashed lines* depict the boundaries of the 'nutrient stream' and *full lines* depict the hydrographic sections used in the analysis; **b** velocity and nitrate flux density along 36° N; **c** volume flux (Sv), and nitrate flux (kmol s^{-1}) along the Gulf Stream (redrawn from Pelegri, JL and Csanady GT, J. Geophys. Res. 96, 2577–2583, 1991, Copyright by the American geophysical Union)

the subpolar gyre and is partly recirculated within the subtropical gyre. Hence, this western boundary flux of nitrate is important in maintaining elevated nitrate concentrations over the subpolar gyre.

The western boundary flux of the upper waters also includes an overturning contribution, which balances the export or import of dense water into the basin. The gyre and overturning contributions to the volume and heat fluxes within the western boundary reinforce each other over the North Atlantic, but oppose each other over the North Pacific. Whether the associated boundary current contributions to the nutrient flux reinforce or op-

pose each other depends on the nutrient distributions. For the North Atlantic, the nutrient fluxes associated with the gyre and overturning circulations oppose each other (Fig. 2.6; Rintoul and Wunsch 1991), but elsewhere either response might occur.

2.4.6 Summary

The combination of gyre and overturning circulations, and patterns of convection determine the large-scale contrasts in nutrient concentration and biological production within ocean basins. The gyre-scale circulation transfers fluid both horizontally and vertically between the thermocline and mixed layer. This transfer leads to the surface waters being nutrient rich over the subpolar gyre and nutrient poor over the subtropical gyre. Nutrients are transferred between each gyre through western boundary currents, Ekman and time-varying eddy circulations.

2.5 Smaller-Scale Circulations: Mesoscale Eddies, Waves and Sub-Mesoscale Fronts

Until recently the nutrient supply to the euphotic zone has been considered primarily in terms of the large-scale, time-mean circulation and diapycnic mixing. However, there is an energetic, time-varying circulation, particularly associated with mesoscale eddies and sub-mesoscale fronts. For example, Fig. 2.15 shows a snapshot of the chlorophyll distribution (derived from Coastal Zone Colour Scanner data) in the Northwest Atlantic Ocean. This snapshot reveals signatures of a range of physical processes: the meandering of the Gulf Stream, the formation of mesoscale eddies and finer-scale frontal filaments drawn out between the larger-scale circulations.

2.5.1 Formation of Mesoscale Eddies and Sub-Mesoscale Fronts

2.5.1.1 *Mesoscale Eddies*

Ocean eddies are formed predominately through baroclinic instability of boundary currents and density fronts. Baroclinic instability occurs preferentially on the scale of the internal Rossby radius of deformation, $L_d = NH/f$, which is typically 30–50 km in the open ocean; here N is the buoyancy frequency, f is the Coriolis parameter and H is a typical thickness scale for the motion. In the ocean, these eddies are usually referred to as mesoscale features, although they are dynamically analogous to atmospheric synoptic-scale, weather sys-

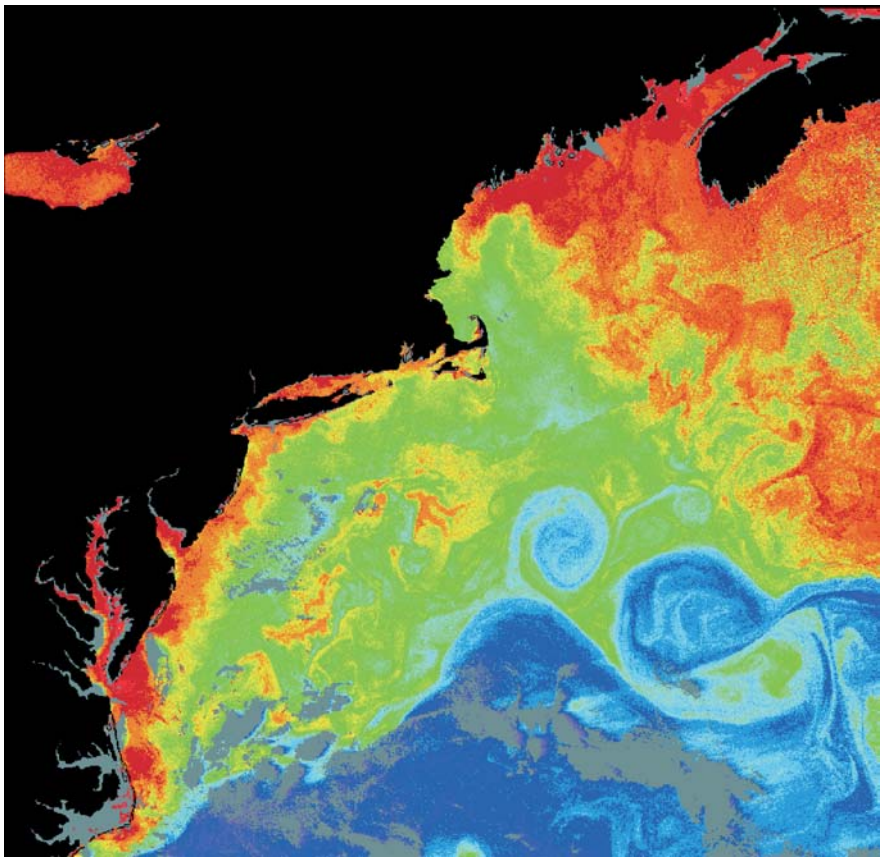

Fig. 2.15.
Chlorophyll picture derived from CZCS over the Northwestern Atlantic. Higher concentrations of chlorophyll (*red*) are evident along the coastal boundary and at higher latitudes. Lower concentrations (*blue*) correlate with the Gulf Stream boundary, the subtropical gyre and anticyclonic eddies. Note the range of physical processes revealed here including boundary currents, mesoscale eddies and finer-scale fronts and filaments (figure courtesy of NASA)

tems. See Rhines (2001) for a brief review of mesoscale eddies, Green (1981) and Gill et al. (1974) for physical descriptions of the instability process and energetics for the atmosphere and ocean respectively.

Baroclinic instability involves a slantwise exchange of fluid across a jet or frontal zone. Available potential energy is released through isotherms being flattened: warm, light fluid rises and is replaced by colder, dense fluid (Fig. 2.16a). For a poleward decrease in temperature, this slantwise exchange leads to the warm fluid rising and moving poleward, and cool fluid sinking and moving equatorward, such that there is a poleward eddy heat flux. In the growth phase of a baroclinic eddy, meanders develop with the rising warm fluid occurring downstream of the trough (region of low pressure) and sinking cold fluid occurring downstream of the ridge (region of high pressure) (Fig. 2.16a). The meanders of the jet amplify and may break off as warm-core, anticyclonic and cold-core, cyclonic eddies, which preferentially occur on the colder and warmer sides of the jet respectively.

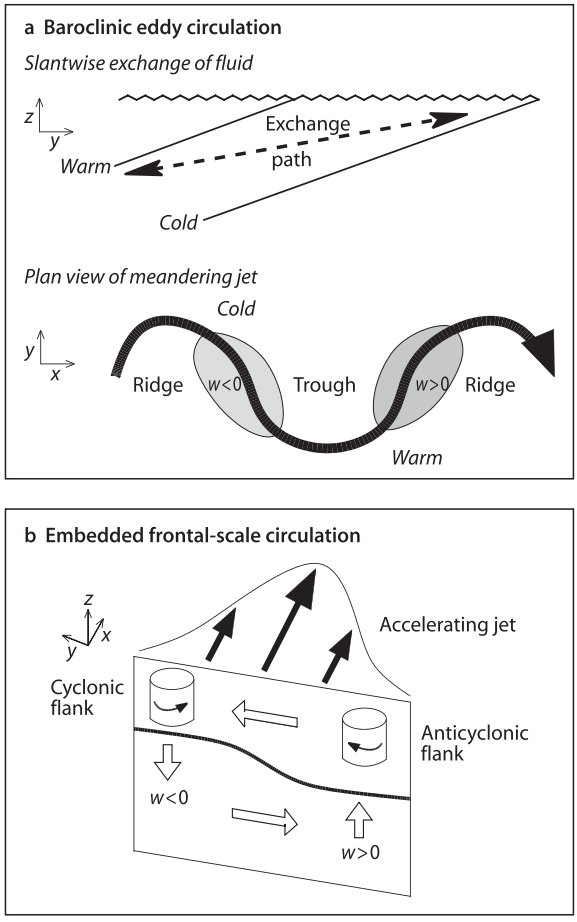

Fig. 2.16. Schematic figure for **a** baroclinic eddy and **b** frontal-scale circulations. In **a**, baroclinic instability releases available potential energy through the flattening of isotherms. This flattening is achieved by a slantwise transfer, as depicted by the *dashed arrow*. For a jet with cooler fluid on the polewards flank, baroclinic instability leads to warm fluid rising and moving polewards downstream between the trough (low pressure) and ridge (high pressure). Conversely, cold fluid sinks and moves equatorwards downstream between the ridge and trough. Eventually, the meanders may develop and form cut-off eddies. The cold-core, cyclonic eddies are formed on the warm flank of the jet and warm-core, anticyclonic eddies on the cold flank. In **b**, frontal-scale circulations are often embedded in the eddy-scale circulations. When a jet accelerates, a secondary circulation is excited across the jet with upwelling occurring on the anticyclonic side and downwelling on the cyclonic side. This secondary circulation reverses if the jet decelerates

2.5.1.2 *Sub-Mesoscale Fronts*

Sub-mesoscale features include fronts and drawn out filaments between mesoscale eddies, as seen in the satellite image in Fig. 2.15. These sub-mesoscale features have a horizontal scale across the flow which is much smaller than the internal Rossby radius of deformation, L_d. When the flow along a jet accelerates, a secondary circulation develops across the jet leading to upwelling on the anticyclonic side and downwelling on the cyclonic side[(6)]. In turn, when the flow along the jet decelerates, a secondary circulation of the reverse sign is formed.

The frontal response may also be understood in terms of conservation of a dynamical tracer, potential vorticity defined by $(\zeta + f)/h$ where h is the thickness of an isopycnic layer, $\zeta = \partial v/\partial x - \partial u/\partial y$ and $f = 2\Omega \sin\theta$ are the vertical components of relative and planetary vorticity respectively; u and v are the eastwards and northwards velocities, Ω is the Earth's angular velocity and θ is the latitude. When a jet accelerates, the absolute vorticity, $\zeta + f$, increases on the cyclonic side of the front and decreases on the anticyclonic side. Consequently, the layer thickness h increases (or decreases) wherever the absolute vorticity, $\zeta + f$, increases (or decreases) in order to conserve potential vorticity. Hence, for the upper ocean, there is downwelling on the cyclonic side and upwelling on the anticyclonic side of a front (Fig. 2.16b). This frontal circulation is discussed further by Woods (1988), as well as for observed ocean case studies by Voorhis and Bruce (1982), and Pollard and Regier (1992).

2.5.2 Local Response to Planetary Waves, Eddies and Fronts

2.5.2.1 *Rectified Transfer of Nutrients into the Euphotic Zone*

A time-varying flow can provide a rectified transfer of nutrients into the euphotic zone through the asymmetrical response of the ecosystem. Over the upper ocean, there is a usually an increase in nutrient concentrations with depth and, in regions such as the subtropical gyres, the euphotic zone is depleted in nutrients by biological export. Undulating motions associated with the time-

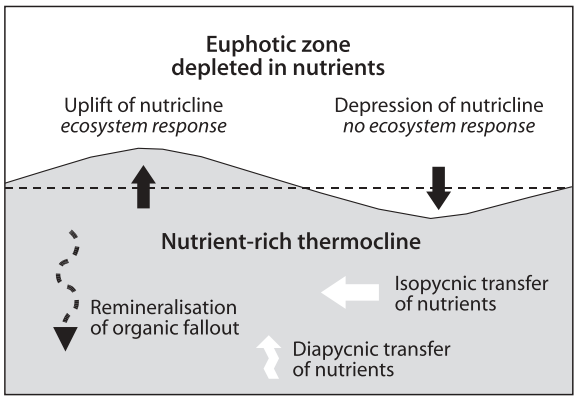

Fig. 2.17. Schematic figure depicting the ecosystem response to an uplift and depression of the nutricline. When nutrient-rich isopycnals are raised into the euphotic zone, there is biological production. Conversely, when the nutrient-rich isopycnals are pushed into the dark interior, there is no biological response. In order for the transient upwelling to persist, there needs to a process maintaining the nutrient concentrations in the thermocline, which might be achieved by remineralisation of organic fallout, diapycnal transfer or a lateral influx of nutrients from the time-mean or time-varying circulations. The schematic figure is generalised from that of McGillicuddy and Robinson (1997)

varying flow can lift nutrient-rich isopycnal surfaces into and out of the euphotic zone. When the isopycnal surface is lifted into the euphotic zone, their illumination may result in photosynthesis and the production of organic matter. In contrast, there is no biological response when the isopycnal surface with nutrient-rich waters is pushed out of the euphotic zone. Consequently, a net biological production can occur as aresult of the time-varying flow(7). This rectification occurs as long as there is sufficient time for the phytoplankton, which have a doubling timescale of typically one day, to respond to an increased nutrient supply, and provided that all the necessary trace elements are available. This process is depicted in Fig. 2.17; the figure is a generalised version of the schematic by McGillicuddy and Robinson (1997) to include horizontal, as well as vertical transfer. Examples of elevated nutriclines and enhanced biological production in cyclonic eddies are provided by Falkowski et al. (1991) and McGillicuddy and Robinson (1997).

2.5.2.2 *Planetary Wave Signals*

The passage of planetary waves and tropical waves might induce rectified upwelling of nutrients. Uz et al. (2001) and Cipollini et al. (2001) identify signatures of planetary waves in surface chlorophyll observations at latitudes less than 40°. There is a westward propagation of surface chlorophyll anomalies and, more importantly, a more rapid propagation towards the equator. These features are broadly consistent with wave theory; e.g. see a review by Killworth (2001). However, it is presently unclear how these chlorophyll signals should be interpreted: the planetary waves might induce enhanced biological production through the rectified upwelling of nutrients into the euphotic zone or the signals might simply be due to a vertical or horizontal advection of existing chlorophyll anomalies.

2.5.2.3 *Mesoscale-Eddy Signals from Baroclinic Instability*

Baroclinic instability leads to the formation of cyclonic eddies with a raised thermocline and anticyclonic eddies with a depressed thermocline. *If* the nutricline and thermocline are coincident, then enhanced production is expected in cyclonic eddies (in accord with the schematic in Fig. 2.17).

The raised thermocline and associated nutricline in a cold-core, cyclone formed by baroclinic instability is *not* due to a simple vertical transfer, since cold fluid sinks and warm fluid rises in slantwise exchange (Fig. 2.16a). Instead in the background environment, the thermocline and associated nutricline have to be raised on the cold side of a frontal zone and depressed on the warm side. Consequently, cyclones acquire their signature of a raised thermocline and nutricline through their *horizontal* movement to a new warmer environment. Likewise, the depressed thermocline and nutricline in an anticyclone is due to its movement into a new colder environment.

Lévy et al. (2001) conduct a careful model study of the instability of a jet, examining where fluid upwells and identifying the biogeochemical response for a range of model resolutions. In their study, they initialise the model with a flat nutricline and integrate for 24 days. For a mesoscale resolution of 6 km, they find enhanced new production occurring preferentially in an anticyclonic eddy and anticylonic filaments where there is upwelling (Fig. 2.18, upper panel). Here, they only find a weaker response for a cyclonic eddy.

Consequently, in our view, baroclinic instability leads to an enhancement of biological production in cyclones due to the *lateral* transfer of cold, nutrient-rich waters, rather than a vertical transfer. However, there is a range of other processes which might provide a direct vertical transfer of nutrients. If instead of baroclinic instability, the cyclones are generated by the interaction of the large-scale flow and topographic features (as speculated by Falkowski et al. 1991), then a vertical uplift of the nutricline should provide enhanced production (Fig. 2.17). There might also be eddy-eddy interactions (as speculated by McGillicuddy and Robinson 1997), which in some cases might intensify features and lead to a local uplift of the nutricline. In addition, there might be enhanced production associated with the vertical contributions from smaller-scale, frontal upwelling (discussed subsequently).

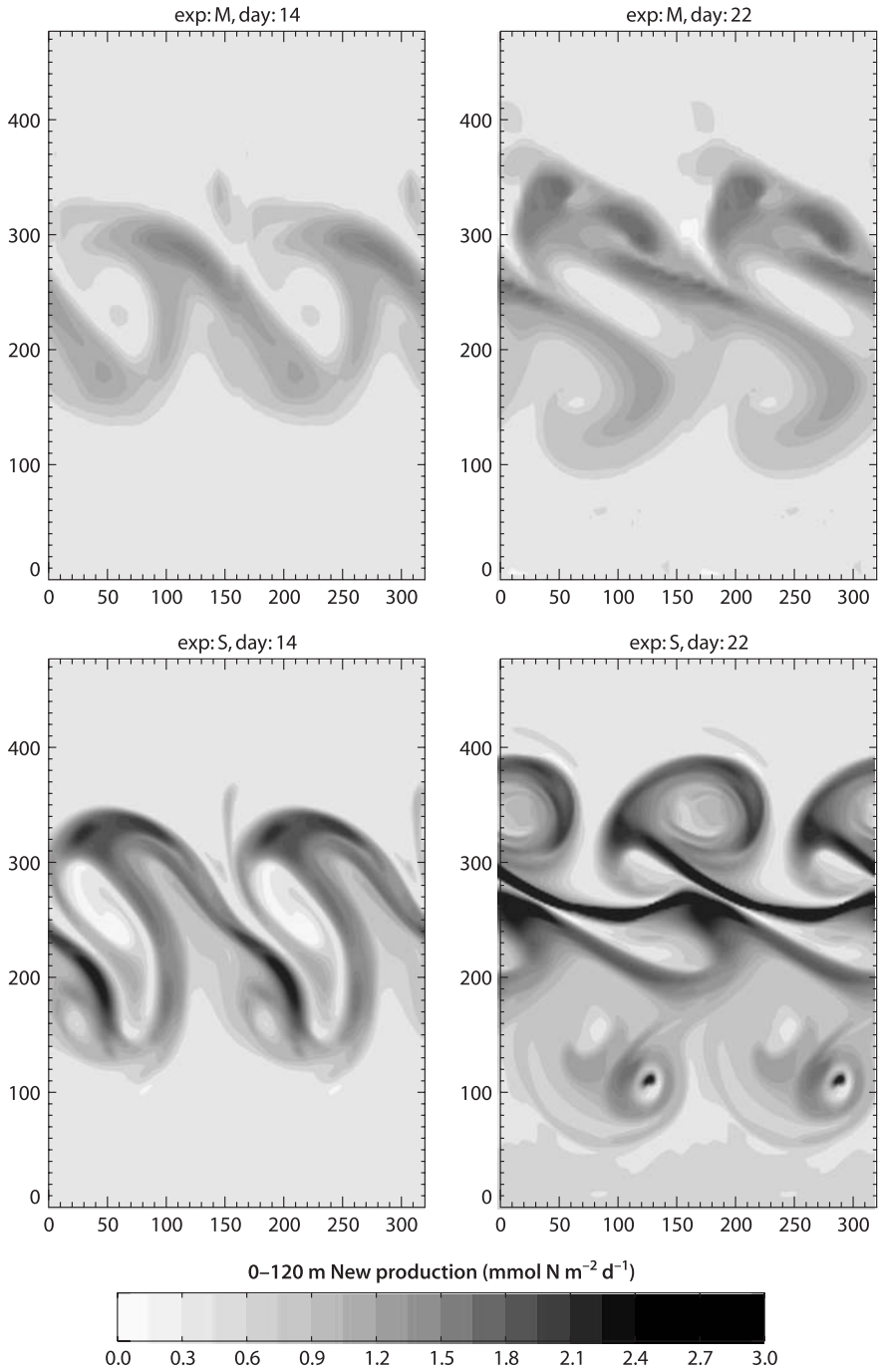

Fig. 2.18.
Modelled new production (10^{-3} mol N m^{-2}) within the euphotic layer for a zonal jet undergoing baroclinic instability (Lévy et al. 2001). Snapshots of the new production are shown at days 14 and 22 for integrations at mesoscale (*upper panel*) and sub-mesoscale (*lower panel*) resolutions of 6 km and 2 km respectively. Over the integration, meanders develop leading to anticyclones to the north and cyclones to the south of the jet. The new production increases in intensity as the resolution increases and becomes concentrated along anticyclonic filaments. The area-averaged new production increases from 6.5 to 10.7 × 10^{-3} mol N m^{-2} as the resolution is increased from 6 km to 2 km; in comparison, the area-averaged new production only reaches 3.7 × 10^{-3} mol N m^{-2} if the resolution is reduced to 10 km

Eddies can also alter the ecosystem by changing the mixed-layer structure and hence altering the light limitation for phytoplankton. Baroclinic slumping of fronts leads to an increase in the stratification and hence a reduction in the thickness of the mixed layer; see modeling studies by Visbeck et al. (1996), Lévy et al. (1998) and Nurser and Zhang (2000). This eddy-induced shallowing can then lead to an onset of a spring bloom prior to the buoyancy input from the atmosphere (Lévy et al. 1998).

2.5.2.4 *Frontal-Scale Signals*

Frontal-scale circulations can also lead to a rectified supply of nutrients to the euphotic zone, since there is upwelling on the anticyclonic side and downwelling on the cyclonic side of an accelerating jet. The observational support for this process acting in the ocean is rather indirect, although maxima in surface chlorophyll have been observed on the anticyclonic side of fronts (Strass 1992).

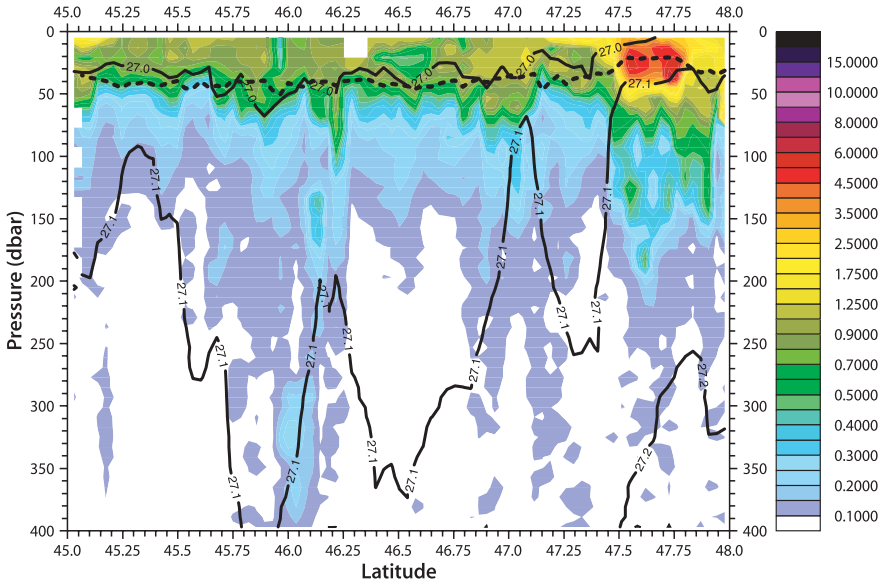

Fig. 2.19.
A vertical section of chlorophyll concentration from the Vivaldi cruise through the eastern North Atlantic in spring 1991. The filaments of chlorophyll extend below the euphotic zone and mixed layer to a depth of up to 400 m and so cannot be formed by convection. Instead the filaments might be formed through frontal subduction occurring on a horizontal scale of 10 km (reprinted from Nurser AJG and Zhang JW, J. Geophys. Res. 105, 21851–21868, 2000, Copyright by the American Geophysical Union)

In addition, plumes of short-lived chlorophyll have been observed penetrating up to 400 m in the stratified thermocline on a horizontal scale of several tens of kilometres (Fig. 2.19). These chlorophyll plumes cannot be formed by convection as they penetrate below the mixed layer. Instead they are consistent with frontal-scale subduction occurring on the cyclonic side of an accelerating front (Fig. 2.16b). This response is analogous to frontal subduction in the atmosphere (Follows and Marshall 1994): ozone-rich stratospheric air is transferred into the weakly stratified, troposphere and assimilated into the troposphere through diabatic forcing (Danielson 1968).

Modeling studies suggest that there is a marked increase in biological activity when frontal circulations are resolved (e.g. Flierl and Davis 1993; Spall and Richards 2000; Mahadevan and Archer 2000; Lévy et al. 2001). The enhancement in biological production is more pronounced at the frontal scale than the ocean eddy scale. For example, the idealised experiments by Lévy et al. (2001) reveal increased levels of new production (and phytoplankton concentration) when the model resolution is increased from 6–2 km (compare upper and lower panels respectively in Fig. 2.18). In the higher-resolution integration, the maxima in new production becomes concentrated at the edges of the anticyclonic eddy, in the anticyclonic area surrounding the cyclonic eddy and within narrow anticyclonic filaments. This response is consistent with the frontal dynamics discussed in relation to Fig. 2.16b. In addition, in a more realistic environment in the vicinity of BATS, Mahadevan and Archer (2000) also demonstrate that there is enhanced nutrient supply to the euphotic zone as the sub-mesoscale is resolved for integrations lasting 120 days (Fig. 2.20).

Specific questions remain though as to how the frontal response alters the productivity over a larger basin scale and the extent that the initial enhancement is sustained over many eddy lifetimes?

2.5.2.5 *Maintenance of Rectified Supply of Nutrients*

The rectified supply of nutrients to the euphotic zone by the time-varying circulations is an appealing mechanism to sustain the export productivity of oligotrophic gyres. Estimates of the eddy supply of nitrate in the Sargasso Sea, based on a combination of hydrographic observations and satellite altimetry, typically reach 0.19 ± 0.10 mol N $m^{-2}\,yr^{-1}$ (McGillicuddy et al. 1998) and 0.24 ± 0.10 mol N $m^{-2}\,yr^{-1}$ (Siegel et al. 1999). These estimates are significant and might help bring estimates of nitrate supply into consistency with estimates of export production inferred from oxygen utilisation and 'age' tracers (Jenkins 1982).

If the rectified supply of nutrients is indeed a dominant process and involves a vertical transfer (irrespective of whether it is due to planetary waves, mesoscale eddies or sub-mesoscale fronts), then this raises the question of how the underlying nutrients in the thermocline are maintained? If the nutrients in the thermocline are *not* maintained, then any rectified supply will only provide an *initial* enhancement in productivity, which will gradually decreases in time until an equilibrium state is reached with lower productivity. This issue is directly analogous to the limited role convection plays in sustaining biological production over several years; see discussion related to Eq. 2.1 to 2.3.

McGillicuddy and Robinson (1997) speculate that an eddy-induced, upwards transport of inorganic nutrients is balanced locally by remineralisation of the downwards flux of sinking organic matter over eddy lifetimes lasting typically a year. However, this local vertical balance cannot hold on longer timescales if any subsequent remineralisation of organic matters occurs at depths greater than the vertical scale for the eddy displacement

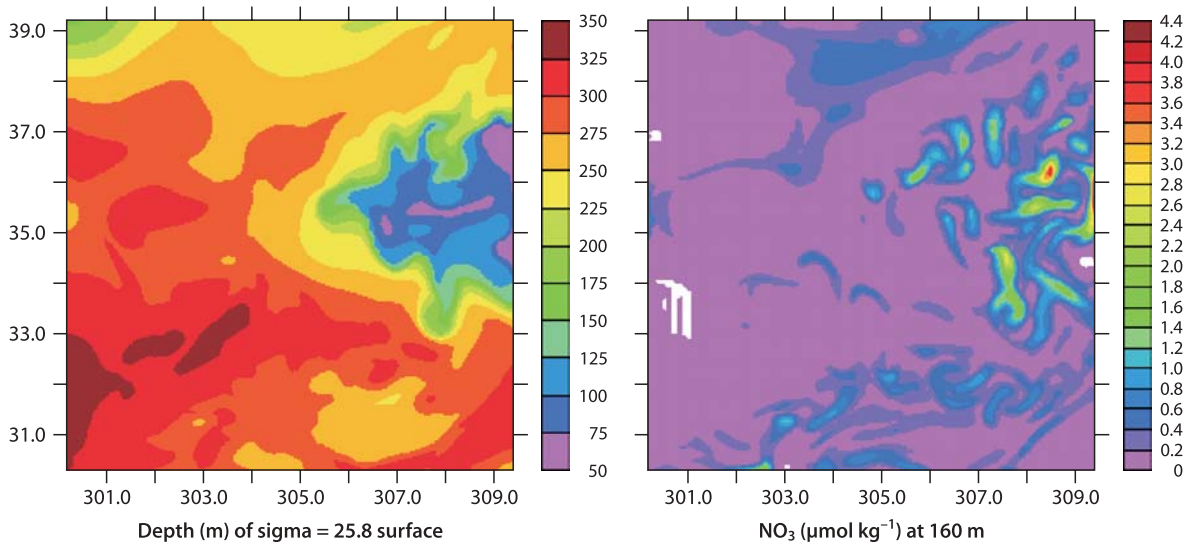

Fig. 2.20. A model simulation of the height of an isopycnal surface and nitrate concentration at a sub-mesoscale resolution of 0.1° integrated at 30–40° N, 50–60° W in the vicinity of the BATS site (Mahadevan and Archer 2000). The model is initialised and forced at the boundaries using output from a global circulation model, with nitrate initialised with data from the BATS, and the regional model integrated for 3 months. The simulation includes folds and frontal-scale undulations in the isopycnal surface. The modelled nitrate concentration reaches a maximum value of 4.3 μmol kg^{-1} at a resolution of 0.1°, which decreases to 1.4 μmol kg^{-1} when the resolution is reduced to 0.4° (not shown here). Hence, this model study suggests that the vertical transport of nitrate takes place primarily at frontal scales, rather than through larger mesoscale features (reprinted from Mahadevan A and Archer D, J. Geophys. Res 105, 1209–1225, 2000, Copyright by the American Geophysical Union)

of isopycnals. In our view, the concentration of nutrients in the upper thermocline are maintained through the *lateral* transport and diffusion of nutrients along isopycnals from surrounding nutrient-rich regions, such as the tropics or subpolar gyre, together with contributions from upwards diapycnal transfer and remineralisation of organic fallout (Fig. 2.17).

2.5.3 Far Field Effects: Eddy Transport and Diffusion

While eddies may provide important *local* impacts on nutrient supply and the ecosystem, they also provide a far field effect. Eddies systematically transfer heat, tracers and nutrients laterally along isopycnals. This larger-scale transfer of tracers consists of a diffusion and a rectified advection along isopycnals (e.g. see Andrews et al. 1987; Gent et al. 1995). The diffusion always acts to transfer tracers down gradient, whereas the rectified advection can lead to an up or down-gradient transfer of tracers.

2.5.3.1 *Eddy Transport of Tracers*

Eddies induce a transport through a correlation in the velocity, v, and vertical spacing between isopycnals, h; the eddy transport velocity or 'bolus' velocity is given by $v^* = \overline{v'h'} / \overline{h}$ where the overbar represents a temporal average and a prime represents a deviation from the temporal average. In the idealised example depicted in Fig. 2.21a, there is a greater volume flux directed to the

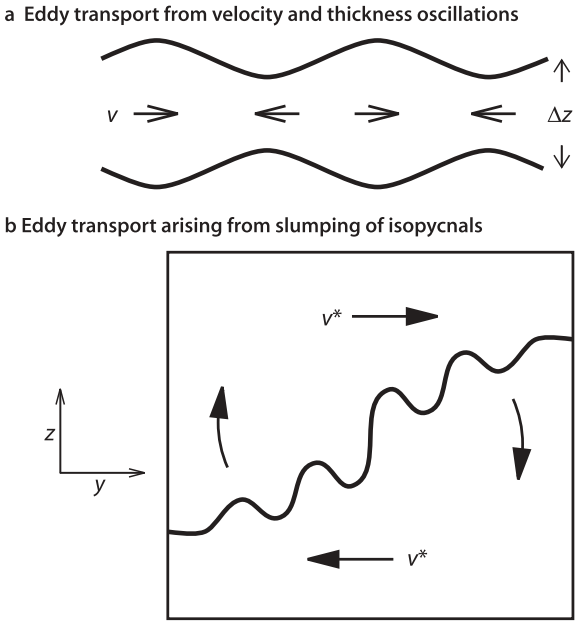

Fig. 2.21. Schematic figure of the eddy-induced transport or 'bolus' velocity, $v^* = \overline{v'h'} / \overline{h}$, for **a** a single layer and **b** a meridional section. The transport arises through a temporal correlation in the velocity, v, and vertical spacing between isopycnals, h, where a prime denotes an eddy deviation and an overbar represents a time average over many eddy events. In **a**, consider an isopycnic layer with no time-mean flow and a layer thickness and velocity oscillating in time. There is a rectified transport whenever the oscillating velocity is correlated with the layer thickness, which is directed to the right as drawn here. In **b**, the eddy-induced advection occurs when there is slumping of the interface, which is usually associated with baroclinic instability (reproduced from Lee et al. (1997))

right than to the left due to the temporal correlation between v and h. The slumping of isopycnals in baroclinic instability generates this rectified transport. For a polewards shoaling of isopycnals, as sketched in Fig. 2.21b, the eddy transport is directed polewards in the surface layer and equatorwards at depth. Conversely, for an equatorwards shoaling of isopycnals, such as on the equatorial side of a subtropical gyre, the eddy transport is directed equatorwards in the surface layer and polewards at depth.

The spreading of a tracer is initially controlled by down-gradient diffusion, but eventually on larger space scales can be controlled by advection[8]; this result is illustrated for idealised tracers and nutrients in eddy-resolving experiments by Lee et al. (1997) and Lee and Williams (2000). The time-varying circulation can lead to different tracer distributions according to whether eddy-induced transport and diffusion either reinforce or oppose each other. The eddy-induced transport is particularly important in controlling the spreading of water masses over the large scale of the Southern Ocean (Danabasoglu et al. 1994; Marshall 1997), as well as across intense and unstable currents, such as the Gulf Stream, and inter-gyre boundaries.

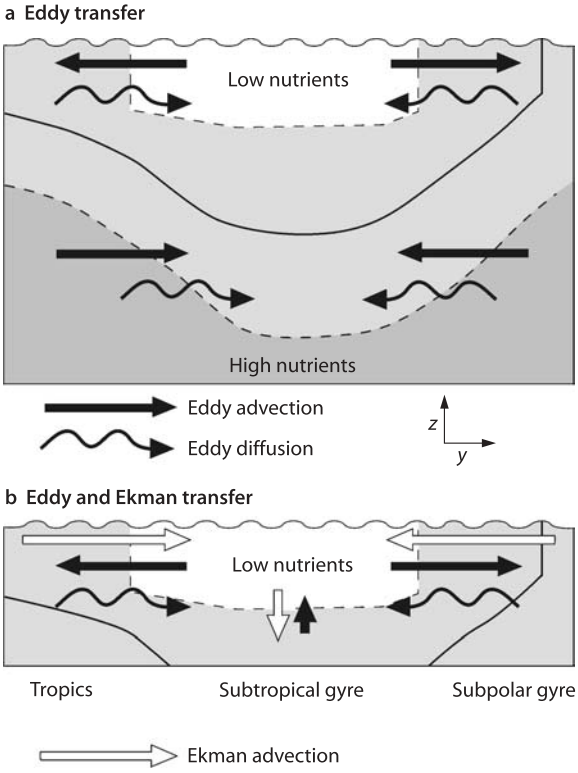

Fig. 2.22. Schematic figure of the eddy-induced nutrient transfer for a subtropical gyre. In **a**, the eddy-induced advection (*black straight arrows*) and diffusion (*curly arrows*) oppose each other at the surface, but reinforces each other at depth. In **b**, the Ekman advection (*white arrow*) is included and dominates over the opposing, eddy-induced advection. Hence, the combination of the eddy and *Ekman transfer* leads to an influx of nutrients into the interior of the subtropical gyre. The same balance should occur over the Southern Ocean where at the surface, there should be a northwards Ekman flux and eddy diffusive transfer of nutrients, which is partially opposed by a southwards eddy-induced advective transfer of nutrients (consistent with the left side of this schematic)

2.5.3.2 *Impact of Eddies on Export Production over the Basin Scale*

On the basin scale, eddies lead to a lateral transport and down-gradient diffusion of nutrients and tracers along isopycnals, which may be important in determining regional nutrient budgets. Eddy transport acts to flatten isopycnals and stratify the water column (Fig. 2.21). Consequently, the eddy transport will only increase biological production *if* the flattening of isopycnals brings nutrients to the surface. This possibility is unlikely to occur over the basin scale, since inorganic nutrient concentrations generally increase with density over the upper ocean (as revealed by gyre-scale undulations of the nutricline reflecting those of the pycnocline).

For a subtropical gyre, eddy diffusion and Ekman transfer should supply nutrients to the euphotic zone (Fig. 2.22, black curly and white arrows respectively). Conversely, the eddy transport should *reduce* the nutrient supply to the euphotic zone and inhibit biological production (Fig. 2.22, black straight arrows), while enhancing the lateral influx of nutrients at depth, and help to maintain nutrient concentrations within the thermocline.

For the North Atlantic, the eddy enhancement of export production over the basin scale has been examined over the basin scale using a simplified ecosystem model coupled with eddy-permitting circulation models at 1/3° (Oschlies and Garçon 1998; Garçon et al. 2001) and 1/9° horizontal resolution (Oschlies 2002). Resolving (at least partially) the eddy mesoscale leads only to a modest enhancement in export production of typically 1/3 over the subtropical gyre. This enhancement is principally achieved through an eddy vertical transfer around the Gulf Stream and an eddy horizontal transfer along the flanks of the subtropical gyre (Oschlies 2002). The inclusion of finer eddy scales also leads to a shallowing of the mixed layer, which reduces the convective supply of nutrients. Further modeling studies are needed to identify how the response over the basin scale alters as submesoscale fronts are fully resolved.

2.5.4 Summary

Fine-resolution observations and modeling studies suggest that nutrient supply by the time-varying circulation supports a significant fraction of biological production, although basin-scale integral estimates of their contribution are difficult to obtain. The time-varying circulation modifies the nutrient distributions and

biological production on a local scale through a rectified transfer of nutrients into the euphotic zone and a modification of the mixed-layer cycle. The rectified transfer involves a horizontal, as well as a vertical transfer of nutrients. There are signals associated with both mesoscale and sub-mesoscale frontal features, but it is presently unclear as to their relative importance and the extent that any initial enhancement is sustained over many eddy lifetimes. On horizontal scales larger than the mesoscale, eddies provide a rectified volume transport and diffusion of nutrients along isopycnals, which might be crucial over the Southern Ocean and across inter-gyre boundaries.

2.6 Interannual and Long-Term Variability

The effect of physical processes on nutrient distributions and biological production has been emphasised in terms of a steady-state view. However, there is clearly significant interannual variability of both the physical processes and the biological cycling. Interannual variability in physical forcing might alter the nutrient or trace metal supply, which in turn can lead to changes in biological production or in the ecosystem through shifts in community structure. However, other ecosystem changes might occur independently of the physical forcing, for example, from result of complex, non-linear interactions in the ecosystem.

2.6.1 Coupled Atmosphere-Ocean Changes: ENSO

The most striking pattern of interannual climate change is El Niño-Southern Oscillation (ENSO) of the tropical Pacific which has far reaching climatic effects around the globe; see reviews by Philander (1990) and Godfrey et al. (2001). This coupled ocean-atmosphere phenomenon, ENSO, is characterised in the oceans by a reduction of the normal Eastern Pacific tropical upwelling related to changes in wind patterns, together with the formation of an anomalously warm surface layer and deep thermocline in the region. These physical changes have a significant impact on the biogeochemical system of the Pacific Ocean and beyond. For example, Fig. 2.23 illustrates the strong contrast in the standing stock of Equatorial Pacific chlorophyll between the January 1998 (El Niño) and January 1999 as observed from the SeaWiFS remote platform.

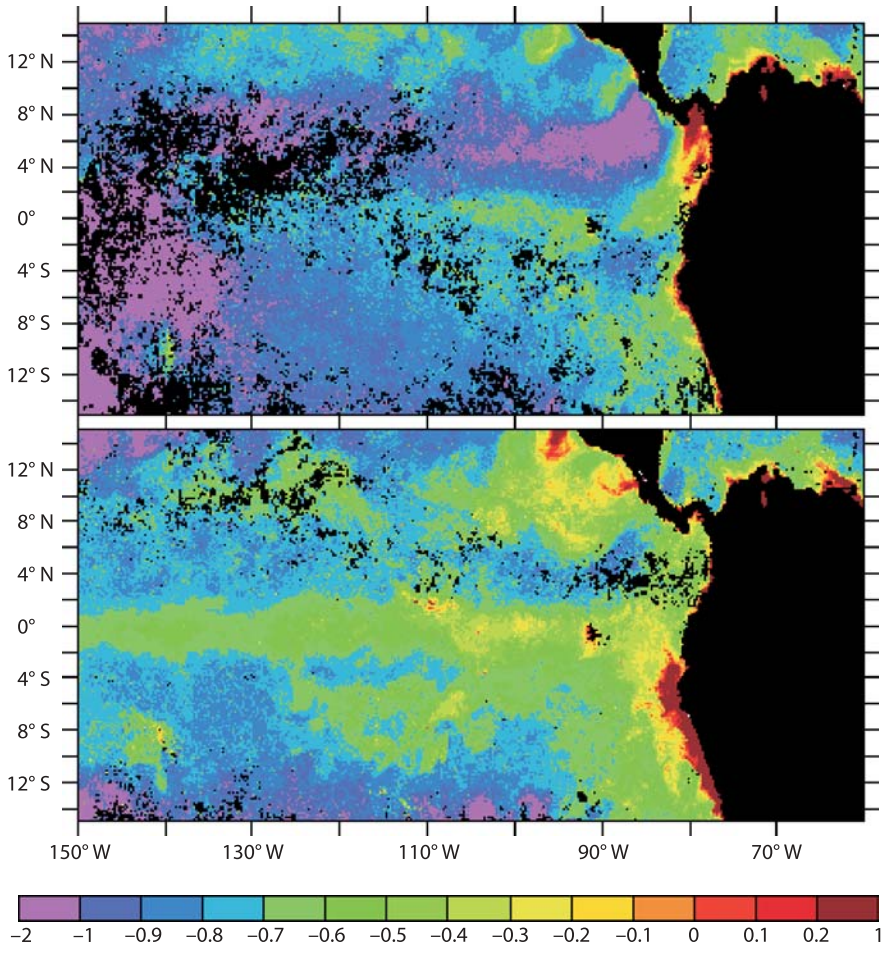

Fig. 2.23. December–January composites of Eastern Pacific chlorophyll derived from SeaWiFS ocean colour observations (level 3 processing). The *upper panel* is for 1997–1998 (during a strong El Niño event), and the *lower panel* is for 1998–1999. Note the suppressed chorophyll concentrations along the equator during the El Niño, corresponding to reduced equatorial and coastal upwelling, a warm sea-surface temperature anomaly, and depressed thermocline and nutricline (data courtesy of NASA)

In 'normal' periods the surface waters of the eastern Equatorial Pacific are relatively cool and rich in macro-nutrients, sustained by a narrow band of equatorial and coastal upwelling of nutrient bearing waters, and relatively inefficient biological export. Consequently, there is typically a band of enhanced chlorophyll associated with the upwelling region (Fig. 2.23, *lower panel*). Modeling studies have emphasised the important role of the Equatorial Undercurrent (EUC) which advects cool, oxygenated waters eastwards at depths of a few tens to hundreds of metres as part of the closure of the wind-driven upper ocean circulation. The EUC is actually depleted in nutrients relative to the adjacent waters on the isopycnic surfaces, but enriched relative to the equatorial surface. Vertical mixing brings nutrients from the EUC to the surface, sustaining local productivity (Toggweiler and Carson 1995; Chai et al. 1996). The relative inefficiency of the biological drawdown of macro-nutrients in the region, and the presence of an HNLC (High Nutrient Low Chlorophyll) regime, may be due to iron limitation. The EUC is also a source of iron to the surface Equatorial Pacific (Coale et al. 1996), although it remains depleted in iron relative to the macro-nutrients. Due to its complex biogeochemical cycling and significant atmospheric and geothermal sources (Christian et al. 2002), the role of iron is, as yet, not fully understood.

During an El Niño event, the easterly Trade Winds are reduced in strength with the equatorial and coastal upwelling weakened or suppressed; the thermocline, nutricline and EUC become anomalously deep. Consequently, the supply of macro-nutrients and iron to the surface from the upwelling and EUC is reduced. In the 1997/1998 El Niño event, even the macro-nutrients eventually became depleted in the region and the chlorophyll concentrations became very low (Fig. 2.23, *upper panel*) (Chavez et al. 1998; Chavez et al. 1999; Murtugudde et al. 1999).

El Niño events occur at irregular intervals of about three to seven years presently, but their frequency and intensity varies on decadal and longer timescales. This longer-term variability may have consequences for nutrient supply and community structure in the Pacific Basin. In this context, there may have been an abrupt shift in the ecosystem of the North Pacific subtropical gyre, during the past 30 years, which has shifted in favour of nitrogen-fixing micro-organisms (Karl et al. 1995; Karl 1999). It is speculated that such an ecosystem shift might be a consequence of the changing physical environment, though the underlying mechanisms are not yet fully revealed.

2.6.2 North Atlantic Oscillation

There is strong interannual variability over the upper ocean of the North Atlantic, which is associated with atmospheric anomalies and changes in air-sea fluxes (Bjerknes 1964). The interannual changes in sea surface temperature (SST) are probably excited by atmospheric anomalies, since the tendency in SST anomalies correlates with latent and sensible heat flux anomalies (Cayan 1992). The dominant mode of atmospheric variability over the North Atlantic is associated with the North Atlantic Oscillation (NAO) (Hurrell 1995), where the NAO index is defined in terms of a sea-level pressure difference between Iceland and Portugal. A high NAO index correlates with enhanced winter surface heat loss and deep convective mixing over the Labrador Sea (Dickson et al. 1996). The opposite is true during periods of low NAO index with anomalous surface heat loss and enhanced convection over the Greenland Sea and Sargasso Sea.

Interannual changes in the ecosystem have been statistically related to regional climate indicators over the North Atlantic. For example, in situ observations of plankton species in the Northeast Atlantic have been correlated with the NAO index (Aebischer et al. 1990) and the position of the northern wall of the Gulf Stream (Taylor et al. 1992). However, in attempting to correlate changes in the ecosystem and physical forcing, there is an inherent problem in the shortness of the temporal records, which could lead to erroneous conclusions[9].

Notwithstanding this reservation, atmospheric forced changes in convection and circulation should modulate the nutrient supply to the euphotic zone, as well as the irradiance phytoplankton receive in spring. Consequently, there are likely to be interannual changes in new and primary production. Variability in local winter mixing has been observed to alter nutrient supply and primary production in the Sargasso Sea (Menzel and Ryther 1961). Interannual variability is apparent in the mixed-layer thickness, and surface nutrient and chlorophyll concentrations at BATS (Bermuda Atlantic Time-Series Station; Fig. 2.24).

Bates (2001) examines the decade long record from the BATS and finds a correlation of –0.33 between the annual primary productivity anomaly there and the NAO index. To the extent that it is significant, the negative correlation indicates the enhancement of convection and nutrient supply there associated with negative anomalies of the NAO. In addition, Williams et al. (2000) predict that much of the variability in convective nitrate supply is correlated with the NAO index over the western and central Atlantic (negative and positive correlations respectively), but not over the eastern Atlantic. Their prediction is consistent with the data analysis of Bates (2001). Their model study is based on an array of one-dimensional mixed-layer models forced by a time-series of atmospheric heat fluxes for 25 years over the North Atlantic. The modelled variability is entirely due to the local atmospheric heat fluxes. Therefore, their predicted lack of correlation with the NAO over the eastern Atlantic is due to the basin-scale mode of the NAO only representing 1/3 of the atmospheric variability. Hence, it is important when interpreting biogeochemical records that the projection of the basin-scale NAO mode is known

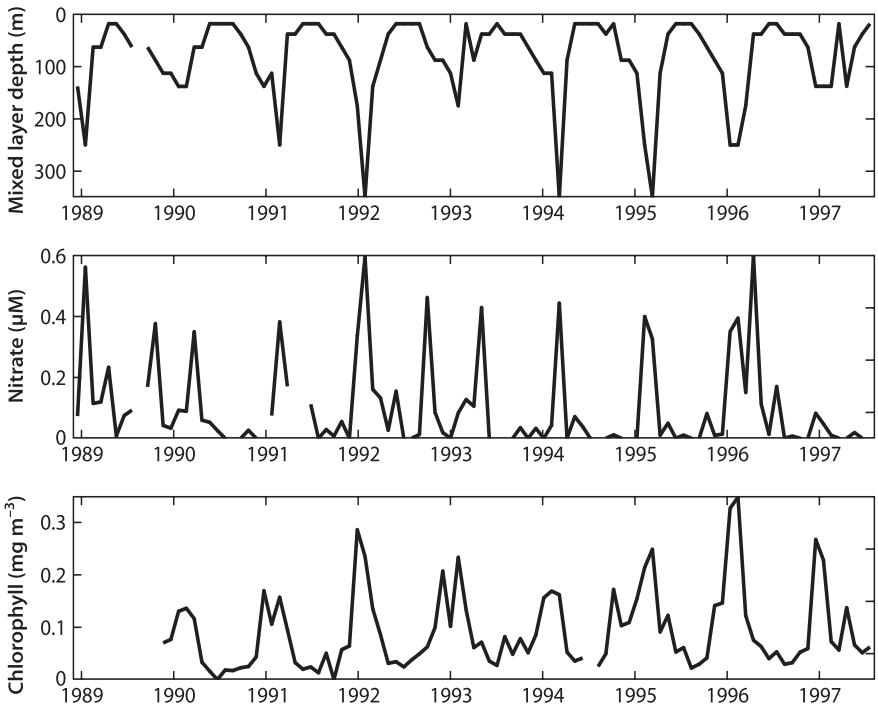

Fig. 2.24.
Time series of **a** mixed-layer thickness (m), **b** nitrate concentration (μmol kg^{-1}) and **c** chlorophyll concentration over the upper 100 m of the water column at the Bermuda Atlantic Time-Series Site (32° N, 65° W) in the North Atlantic subtropical gyre. The mixed-layer thickness is diagnosed by the depth at which the density increases by 0.125 kg m^{-3} from the surface value. The time-series illustrates the interannual variability in winter-time convection and the corresponding influence on the supply of nitrate to the euphotic zone and the response in primary production. For example, the winter-mixed layer is thin in 1990 and thick in 1992, which correlates with reduced and enhanced concentrations in nitrate and chlorophyll respectively (data from BATS)

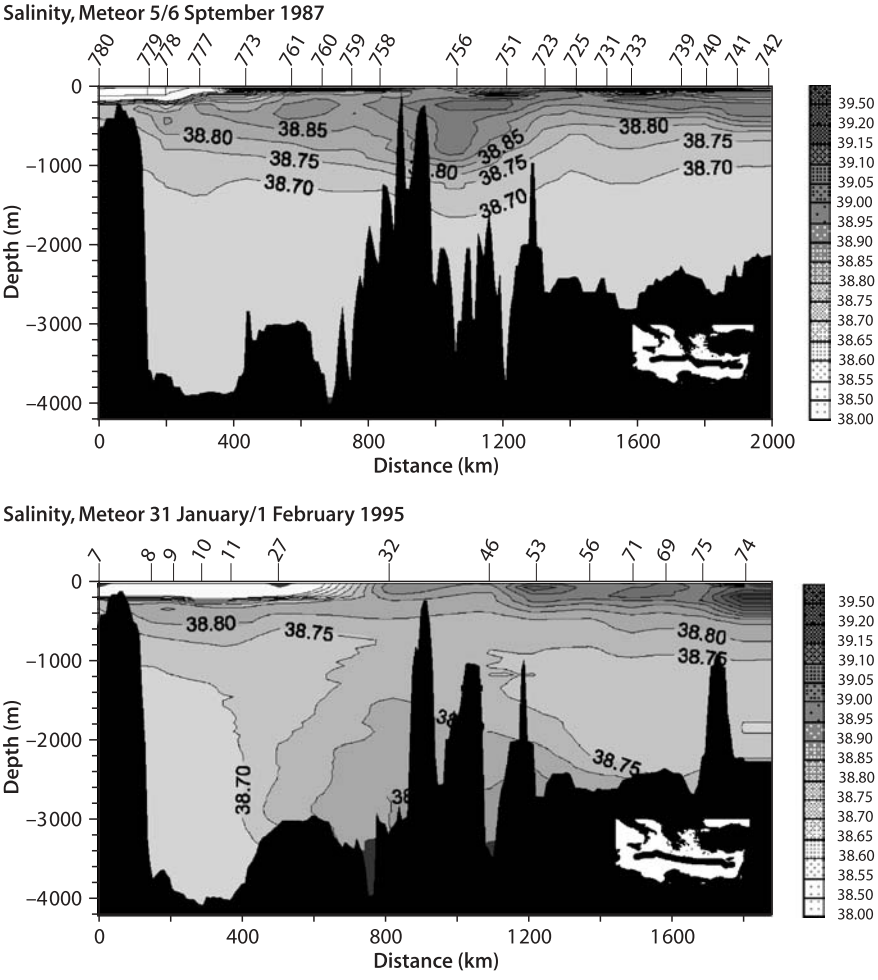

Fig. 2.25.
Deep salinity shift for 1987 (*upper panel*) and 1995 (*lower panel*) for a zonal section through the Eastern Mediterranean (see *inset*). The deep salinity is relatively uniform in 1987, but then dramatically changes by 1995 with an influx of new saline bottom water originating from the Aegean (modified from Roether et al., Recent changes in Eastern Mediterranean deep waters, Science 271, 333–335, Copyright (1996) American Association for the Advancement of Science)

for a particular region, since other more regional atmospheric modes might sometimes become important.

Interannual variations in the spring bloom of the North Atlantic are subject to the same meteorological influences that lead to regional variations illustrated and discussed in Fig. 2.8. In the subtropical gyre, much of the variability in local interannual variations of the spring bloom may be attributed to changes in meteorological forcing (Follows and Dutkiewicz 2002), although other processes, such as mesoscale motions and ecosystem changes probably become more significant at other times of year. In the subpolar gyre, the interannual variability of the spring bloom does *not* appear to exhibit any clear relationship with meteorological forcing due to the dominance of ecosystem changes or the control by mesoscale eddies of the restratification process.

2.6.3 Changes in Overturning Circulation

Major changes in the global overturning circulation might result in dramatic changes in biological production. Here, we discuss two specific examples related to changes in nutrient distributions: a present day, abrupt change over the eastern Mediterranean and a larger-scale, inferred glacial change over the North Atlantic.

2.6.3.1 *Abrupt Change in the Eastern Mediterranean*

A unique present day example of such an overturning shift has occurred in the eastern Mediterranean. There is an internal overturning cell within the eastern Mediterranean with dense waters usually formed in the Adriatic and spreading over the eastern Mediterranean. This mode of deep circulation appears to have persisted over the last century (as implied by hydrographic observations), which has led to the deep water masses being particularly homogeneous. However, between 1987 and 1995, there has been an abrupt change with the Aegean forming the most dense water mass and, temporarily, replacing the Adriatic as the source of bottom water (Roether et al. 1996). This signal is revealed by an influx of warm, salty water at depth across the eastern Mediterranean in 1995 (Fig. 2.25). The resulting uplift of the previous bottom water has moved the nutricline much closer to the euphotic zone (Fig. 2.26)

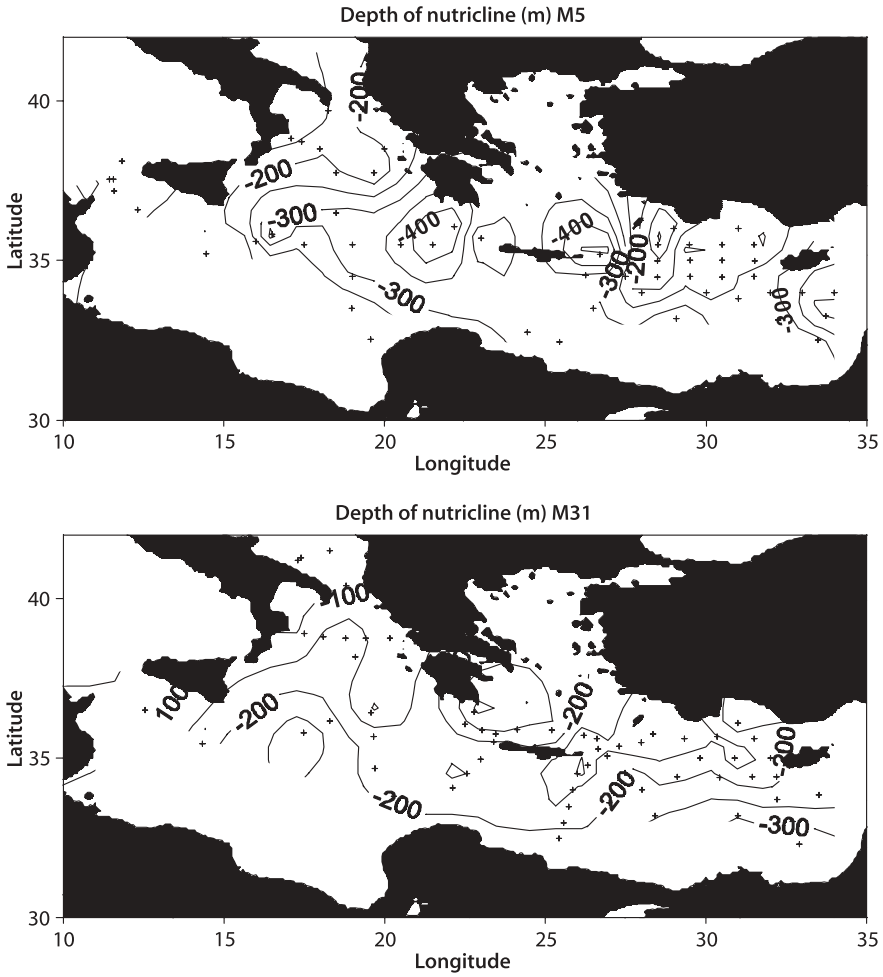

Fig. 2.26.
Nutricline shift (m) for 1987 (*upper panel*) and 1995 (*lower panel*) over the Eastern Mediterranean, which corresponds to the salinity sections shown in Fig. 2.25. The nutricline is defined by the depth below the surface where the nitrate concentration reaches 3 μmol N kg^{-1}. The nutricline is typically 300 m to 400 m deep in 1987, but is uplifted to a depth of 200 m by 1995 following the influx of dense water (reprinted from Deep-Sea Res. 1, 46, Klein B et al., 371–414, Copyright (1999) with permission from Elsevier Science)

(Klein et al. 1999), which provides a 'natural fertilization experiment' for the oligotrophic surface waters. Subsequently, enhanced biological production is likely to occur in the spring following severe winters when there is increased entrainment of nutrient-rich, thermocline waters; a signal of winter-induced, interannual variability in the phytoplankton bloom is observed over the Adriatic (Gacic et al. 2002). Such a localised change might, in principle, occur elsewhere over the global ocean.

2.6.3.2 *Change in the Phosphorus Distribution over the Glacial North Atlantic*

Larger-scale shifts in the nutrient distributions, probably achieved by overturning changes, have also been suggested by the paleo-record in ocean sediments. For example, studies of the cadmium content of benthic foraminifera suggest that the ocean distribution of phosphorus has changed over glacial-interglacial timescales. Variations of cadmium around the ocean are closely correlated with the variations of phosphorus, since the two elements are assimilated into organic matter and regenerated in close accord (Boyle et al. 1976; Boyle 1988). The cadmium is assimilated into calcium carbonate shells, the Cd/Ca ratio reflecting the waters of origin and, in turn, the phosphate concentration.

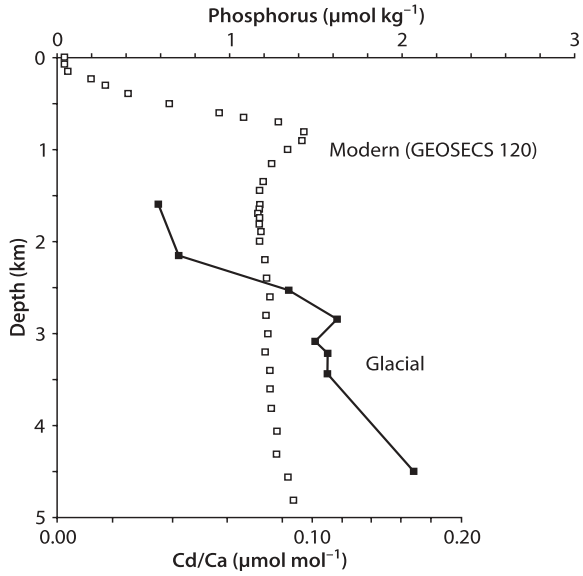

Fig. 2.27. A phosphorus profile representative of the present day, western North Atlantic compared with a glacial profile reconstructed from Cd/Ca ratios of benthic foraminifera in sediment cores (from Boyle and Keigwin 1987). The glacial reconstruction assumes that the Cd-P relationship of the glacial oceans was similar to the present day. The observed Cd-P curve is well represented as two intersecting linear relationships which is reflected in the change of scale on the Cd/Ca axis (see Boyle 1988). The reconstruction suggests a significant increase in the vertical gradient in phosphorus over the North Atlantic during the last glacial period

Boyle and Keigwin (1987) compared a phosphorus profile from the modern western North Atlantic with a reconstruction from Cd/Ca ratios in sediment cores for the last glacial period, as shown in Fig. 2.27. There appears to have been a significant shift in the phosphorus distribution over the North Atlantic with increased concentrations in the bottom waters and an enhanced vertical gradient for the last glacial period. They speculate that these changes are due to variations in the overturning circulation with an increased influx of AABW and a decreased formation of NADW occurring over the last glacial period for the North Atlantic.

2.6.4 Summary

There is marked interannual and longer-term variability in the physical forcing and biogeochemical response over the ocean. This variability can involve coupled atmosphere-ocean interactions, such as ENSO, or atmospheric-triggered changes (with probably little immediate atmospheric feedback) such as NAO. This variability is not only restricted to the upper ocean, but can involve abrupt changes in the deep ocean, as evident in recent changes in the eastern Mediterranean. All of this variability can also occur in the paleo-environment. An important challenge is to interpret both present day and paleo-oceanographic records in terms of physical and biogeochemical mechanisms in a well-constrained manner.

2.7 Conclusions

Ocean circulation, nutrient transports, and biological productivity are intimately linked over a broad spectrum of space and time scales. The physical supply of nutrients and trace metals can sometimes limit the levels of export production. However, even in regions where other processes become limiting, the physical supply of nutrients and trace metals needs to be consistent with the levels of export production for there to be a steady state. Here, we have reviewed the role of physical phenomena, on horizontal scales from global to frontal, in determining nutrient distributions and modulating the supply of nutrients to the euphotic zone over the open ocean. The key points of our review may be summarised as follows:

- The large-scale overturning circulation and its transport of nutrients is the principal physical mechanism determining the nutrient contrasts between ocean basins. Together with the biological fallout and remineralisation of organic matter, the overturning circulation leads to the deep waters of the Pacific and

Indian Oceans having much higher concentrations in inorganic nutrients than the Atlantic Ocean. Separate and independent overturning cells connect each basin with the Southern Ocean.

- Convective mixing acts to transfer nutrients from the seasonal boundary layer into the euphotic zone and is significant in modulating productivity on seasonal and interannual timescales.
- The gyre-scale circulation transfers nutrients both vertically and horizontally within ocean basins. In association with biological consumption and fallout, this advective transfer leads to the surface waters being nutrient rich over subpolar gyres and nutrient poor over subtropical gyres. The western boundary currents and lateral Ekman transfers across the inter-gyre boundaries help to maintain the nutrient concentrations within each gyre.
- Time-varying circulations may locally enhance biological production through rectified transfer of nutrients across the base of the euphotic zone. This fine-scale enhancement can occur at the ocean eddy and frontal scale, and involves both vertical and horizontal advection of nutrients. Eddies also provide a large-scale, rectified volume transport and diffusion of nutrients along isopycnals. This isopycnic transfer is particularly important in determining nutrient distributions over the Southern Ocean and in transferring nutrients across inter-gyre boundaries.
- In addition, these physical phenomena affect the inter-annual and longer-term variability of the biogeochemical system, as evident in changes associated with circulation modes: ENSO and the North Atlantic Oscillation. For example, atmospheric modulation of convection or the circulation might alter the levels of biological production or the state of the ecosystem through changes in nutrient or trace-metal supply.

While we have attempted to provide a mechanistic view of the competing physical processes for the open ocean, we are aware of several difficulties. Firstly, for clarity, we have described each process separately and independently, rather than adopt a purely regional view. However, each process is naturally connected to each other. For example, boundary currents are part of both the gyre and overturning circulations, energetic circulations contain a mixture of eddies and fronts, and atmospheric variability induces changes in convection, circulation and inputs of trace metals. Secondly, the biogeochemical response to the physical processes has only been discussed in a qualitative manner. The lack of quantitative constraints is one of the principal challenges that need to be addressed for both present day and paleo analyses. In assessing the role of different processes, a distinction needs to be made between how important a process is in perturbing the system (such as providing a short-term burst in nutrient supply to the euphotic zone) and in maintaining a long term equilibrium.

Understanding the impact of the present-day variability requires maintenance and further development of long term time-series stations in order to provide a reliable observational context. In addition, regional and global surveys of the organic forms of nutrients are required in order to quantify the fluxes and budgets of the total nutrient pools. Addressing these outstanding issues will be challenging due to the importance of rectified signals in biogeochemistry, such as those involving temporal variations in convection, the mesoscale eddy and frontal circulations. One approach is to adopt an increased use of targeted experiments, combined with models, to identify the observational signals and assess the competing processes.

Acknowledgements

We are grateful to all authors kindly providing copies of their figures, and thank Ed Boyle, Jim Christian, Harry Leach and George Nurser for their feedback. RGW is grateful for support from the UK Natural Environment Research Council (NER/O/S/2001/01245) and MJF is grateful for support from NASA grant NCC5-244.

Notes

1. The diapycnic diffusivity is typically 10^{-5} m^2 s^{-1} in the main thermocline (e.g. Ledwell et al. 1993), but reaches much higher values above rough topography (Polzin et al. 1997) and near coastal boundaries. Munk and Wunsch (1998) argue that the combination of the weak background mixing and localised enhanced mixing might lead to an effective diffusivity of 10^{-4} m^2 s^{-1} acting over the deep ocean. They suggest that this mixing is driven by the mechanical inputs of energy from the winds and tides. However, even with a higher mixing rate over the deep ocean, there is still a difficulty in explaining the nutrient transfer over the upper ocean in terms of diapycnic diffusion and vertical advection by the large-scale circulation.
2. Traditionally, frontal definitions are used to define the regions over which water masses form and spread over the Southern Ocean (Orsi et al. 1995). The surface signatures of fronts are particularly evident in maps of the gradient in sea surface temperature inferred from remotely-sensed observations (Hughes and Ash 2001). These remotely-sensed observations and general circulation model experiments suggest

though that these fronts are *not* always continuous features around the Southern Ocean, but instead merge or separate according to the topography (Pollard et al. 2002).

3. The eddy transport was first discussed in the atmosphere to explain how tracers can be transported in the opposite direction to the time-mean Eulerian circulation; e.g. Andrews et al. (1987). This eddy transport explains the polewards heat transport across the troposphere and cancellation of the 'Ferrel' cell, as well as the transport of ozone-rich, tropical air towards the high latitude, winter hemisphere in the stratosphere. For the Southern Ocean, the dominant eddy contribution across *latitude circles* occurs from standing eddies involving spatial deviations in a zonal average (Döös and Webb 1994; Karoly et al. 1997), although transient eddies control the transfer across time-mean *streamlines* (Hallberg and Gnanadesikan 2001).
4. The eastwards and northwards Ekman volume fluxes are defined by $U = \tau_y / (\rho f)$ and $V = -\tau_x / (\rho f)$ respectively; here τ_x and τ_y are the eastwards and northwards components of the wind stress, ρ is the density and f is the Coriolis parameter. The upwelling at the base of the surface Ekman layer is given by the convergence of the horizontal Ekman flux or equivalently the curl of the wind stress divided by the Coriolis parameter.
5. Model estimates of the lifetime of semi-labile, dissolved organic nitrogen (DON) range from several months in the surface to years in the main thermocline. For example, Anderson and Williams (1999) model the cycling of organic matter and obtain DON lifetimes of 0.4 years at the surface and increasing to 6 years at 1 000 m as the concentration of bacteria decreases with depth.
6. Along a front, there is a balance between the acceleration of the along front velocity, Du/Dt and the cross-frontal Coriolis acceleration, $-fv$, where

$$\frac{Du}{Dt} - fv = 0$$

where, u and v are the velocities aligned along and across the front, f is the Coriolis parameter and D/Dt is the rate of change following a fluid parcel (Eliassen 1962). The secondary circulation associated with the cross-frontal flow satisfies

$$\frac{\partial v}{\partial y} + \frac{\partial w}{\partial z} = 0$$

where w is the vertical velocity. Thus, for an accelerating eastwards jet, $Du/Dt > 0$, then the secondary circulation is with a polewards surface flow ($v > 0$), inducing downwelling ($w < 0$) on the polewards, cyclonic side of the front and upwelling ($w > 0$) on the equatorwards, anticyclonic side of the front; see Newton (1978) for a discussion of both ocean and atmospheric cases.
7. The asymmetrical response of the ecosystem to transient upwelling is directly analogous to the interaction of a time-varying circulation and photochemistry in the stratosphere. Ozone-rich air in the stratosphere survives when transferred towards the darker, winter pole and is destroyed when transferred to the sunlit equator. This asymmetry leads to a rectified transport of ozone towards the winter pole and maximum concentration in total ozone occurring away from its photochemical source.
8. Consider a patch of dye spreading from a localised source through advection and diffusion. Scale analysis suggests that the dye spreads advectively over a spatial scale

$$L_{\text{adv}} \sim Vt$$

where V is the transport velocity including the rectification of the time-varying flow from the correlation of the velocity and layer thickness, and t is time. The dye will also spread diffusively over a spatial scale,

$$L_{\text{dif}} \sim (Kt)^{1/2}$$

where K is the eddy-induced diffusivity of tracer. The ratio of these length scales is

$$\frac{L_{\text{adv}}}{L_{\text{dif}}} \approx \frac{V}{K^{1/2}} t^{1/2}$$

Thus, for non-zero V and K, the initial spreading will be diffusive, since the ratio of $L_{\text{adv}}/L_{\text{dif}}$ is small. Over longer timescales, however, advection becomes important, as the horizontal scales inflate, and may eventually dominate over diffusion. For example, assuming $K \sim 1\,000$ m^2 s^{-1} and $V \sim 1$ cm s^{-1} suggests that advection and diffusion becomes comparable after a timescale of order several years.
9. The issue of misleading correlations arising from the shortness of the time record compared with the period of any oscillations is discussed by Wunsch (1999) in terms of the North Atlantic and Southern Oscillations. In addition, Wunsch (2001) reports on a climate example where the water level of Central African lakes were thought to be correlated with monthly sunspot numbers based on a 20 year record. However, this correlation turned out to be erroneous when the lake record was extended to 70 years and included more cycles in the sunspot numbers.

References

Abell J, Emerson S, Renaud P (2000) Distribution of TOP, TON, and TOC in the North Pacific subtropical gyre: implications for nutrient supply in the surface ocean and remineralisation in the upper thermocline. J Mar Res 58:203–222

Aebischer NJ, Coulson JC, Colebrook JM (1990) Parallel long-term trends across four marine trophic levels and weather. Nature 347:753–755

Anderson TR, Williams PJL (1999) A one-dimensional model of dissolved organic carbon cycling in the water column incorporating combined biological-photochemical dependence. Global Biogeochem Cy 13:337–349

Andrews DJ, Holton JR, Leovy CB (1987) Middle atmosphere dynamics. Academic Press, 489 pp

Archer D, Johnson EK (2000) A model of the iron cycle in the ocean. Global Biogeochem Cy 14:269–279

Backhaus JO, Wehde H, Hegseth EN, Kampf J (1999) 'Phyto-convection': the role of oceanic convection on primary production. Mar Ecol Prog Ser 189:77–92

Barber RT (1992) Geologic and climatic time scales of nutrient variability. In: Falkowski PG, Woodhead AD (eds) Primary productivity and biogeochemical cycles in the sea. Plenum Press, New York, pp 89–106

Bates N (2001) Interannual variability of oceanic CO_2 and biogeochemical properties in the Western North Atlantic Subtropical Gyre. Deep-Sea Res Pt II 48:1507–1528

Behrenfeld MJ, Falkowski PG (1997) Photosynthetic rates derived from satellite-based chlorophyll concentration. Limnol Oceanogr 42:1–20

Bjerknes J (1964) Atlantic air-sea interaction. Adv Geophys, 20, 1–82

Boyle EA (1988) Cadmium: chemical tracer of deepwater paleoceanography. Paleoceanography 3:471–489

Boyle EA, Keigwin L (1987) North Atlantic thermohaline circulation during the past 20 000 years linked to high-latitude surface temperature. Nature 330:35–40

Boyle EA, Sclater FR, Edmond JM (1976) On the marine geochemistry of cadmium. Nature 263:42–44

Broecker WS (1991) The great ocean conveyor. Oceanography 4: 79–89

Cayan DR (1992) Latent and sensible heat flux anomalies over the Northern Oceans: driving the sea surface temperature. J Phys Oceanogr 22:859–881

Chai F, Lindley ST, Barber RT (1996) Origin and maintenance of a high nitrate condition in the Equatorial Pacific. Deep-Sea Res Pt II 43:1031–1064

Chavez FP, Strutton PG, McPhaden MJ (1998) Biological-physical coupling in the central equatorial Pacific during the onset of the 1997–98 El Niño. Geophys Res Lett 25:3543–3546

Chavez FP, Strutton PG, Friedrich GE, Feely RA, Feldman GC, Foley DG, McFaden MJ (1999) Biological and chemical response of the Equatorial Pacific Ocean to the 1997–98 El Niño. Science 286:2126–2131

Christian JR, Verschell MA, Murtugudde R, Busalacchi AJ, McClain CR (2002) Biogeochemical modelling of the tropical Pacific Ocean. II. Iron biogoechemistry. Deep-Sea Res Pt II 49:545–565

Cipollini P, Cromwell D, Challenor PG, Raffaglio S (2001) Rossby waves detected in global ocean colour data. Geophys Res Lett 28:323–326

Coale KH, Fitzwater SE, Gordon RM, Johnson KS, RT Barber (1996) Control of community growth and export production by upwelled iron in the equatorial Pacific Ocean. Nature 379:621–624

Danabasoglu G, McWilliams JC, Gent PR (1994) The role of mesoscale tracer transports in the global ocean circulation. Science 264:1123–1126

Danielsen EF (1968) Stratospheric-tropospheric exchange based on radioactivity, ozone and potential vorticity. J Atmos Sci, 25, 502–518

Denman KL, Gargett AE (1995) Biological-physical interactions in the upper ocean: the role of vertical and small scale transport processes. Annu Rev Fluid Mech 27:225–255

Dickson R, Lazier J, Meinke J, Rhines P, Swift J (1996) Long-term coordinated changes in convective activity of the North Atlantic. Prog Oceanogr 38:241–295

Döös K, Webb DJ (1994) The Deacon cell and the other meridional cells of the Southern Ocean. J Phys Oceanogr 24:429–442

Duarte CM, Agusti S (1998) The CO_2 balance of unproductive aquatic ecosystems. Science 281:234–236

Dutkiewicz S, Follows M, Marshall J, Gregg WW (2001) Interannual variability of phytoplankton abundances in the North Atlantic. Deep-Sea Res Pt II 48:2323–2344

Eliassen A (1962) On the vertical circulation in frontal zones. Geofysiske Publikasjoner, Geophysica Norvegica XXIV:147–160

Emerson S, Quay P, Karl D, Winn C, Tupas L, Landry M (1997) Experimental determination of the organic carbon flux from open-ocean surface waters. Nature 389:951–954

Falkowski PG, Ziemann D, Kolber Z, Bienfang PK (1991) Role of eddy pumping in enhancing primary production in the ocean. Nature 352:55–58

Fasham MJR (1995) Variations in the seasonal cycle of biological production in subarctic oceans; a model sensitivity analysis. Deep-Sea Res Pt I 42:1111–1149

Flierl GR, Davis CS (1993) Biological effects of Gulf Stream meandering. J Mar Res 51:529–560

Follows MJ, Dutkiewicz S (2002) Meteorological modulation of the North Atlantic spring bloom. Deep-Sea Res Pt II 49: 321–344

Follows MJ, Marshall JC (1994) Eddy-driven exchange at ocean fronts. Ocean modelling 102:5–9

Gacic M, Civitarese G, Miserocchi S, Cardin V, Crise A, Mauri E (2002) The open-ocean convection in the Southern Adriatic: a controlling mechanism of the spring phytoplankton bloom. Cont Shelf Res 22:1897–1908

Ganachaud A, Wunsch C (2002) Oceanic nutrient and oxygen transports and bounds on export production during the World Ocean Circulation Experiment. Global Biogeochem Cy, vol. 16, 4:1057

Garçon VC, Oschlies A, Doney SC, McGillicuddy D, Waniek J (2001) The role of mesoscale variability on plankton dynamics in the North Atlantic. Deep-Sea Res Pt II 48:2199–2226

Gent PR, Willebrand J, McDougall TJ, McWilliams JC (1995) Parameterising eddy-induced tracer transports in ocean circulation models. J Phys Oceanogr 25:463–474

Gill AE, Green JSA, Simmons AJ (1974) Energy partition in the large-scale ocean circulation and the production of mid-ocean eddies. Deep-Sea Res 21:499–528

Gnanadesikan A (1998) A global model of silicon cycling: sensitivity to eddy parameterization and dissolution. Global Biogeochem Cy 13:199–220

Godfrey JS, Johnson GC, McPhaden MJ, Reverdin G, Wijffels SE (2001) The tropical ocean circulation. In: Siedler G, Church J, Gould J (eds) Ocean circulation and climate. Academic Press, pp 215–246

Green JSA (1981) Trough-ridge systems as slant-wise convection. In: Atkinson BW (ed) Dynamical meteorology: an introductory selection. Methuen & Co. Ltd, pp 176–194

Gruber N, Sarmiento JL (1997) Global patterns of marine nitrogen fixation and denitrification. Global Biogeochem Cy 11:235–266

Hallberg R, Gnanadesikan A (2001) An exploration of the role of transient eddies in determining the transport of a zonally reentrant current. J Phys Oceanogr 31:3312–3330

Hanawa K, Talley L (2001) Mode waters. In: Siedler G, Church J, Gould J (eds) Ocean circulation and climate. Academic Press, pp 373–386

Hughes CW, Ash E (2001) Eddy forcing of the mean flow in the Southern Ocean. J Geophys Res 106:2713–2722

Hurrell JW (1995) Decadal trends in the North Atlantic Oscillation: regional temperatures and precipitation. Science 269: 676–679

Hutchings L, Pitcher GG, Probyn TA, Bailey GW (1995) The chemical and biological consequences of coastal upwelling. In: Summerhayes CP, Emeis K-C, Angel MV, Smith RL, Zeitzchel B (eds) Upwelling in the ocean: modern processes and ancient records. John Wiley & Sons, New York, pp 65–81

Jackson GA, Williams PM (1985) Importance of dissolved organic nitrogen and phosphorus to biological nutrient cycling. Deep-Sea Res 32:223–235
Jenkins WJ (1982) Oxygen utilization rates in North Atlantic subtropical gyre and primary production in oligotrophic systems. Nature 300:246–248
Jenkins WJ (1988) Nitrate flux into the photic zone near Bermuda. Nature 331:521–523
Jenkins WJ, Goldman JC (1985) Seasonal oxygen cycling and primary production in the Sargasso Sea. J Mar Res 43:465–491
Karl DM (1999) A sea of change: biogeochemical variability in the North Pacific subtropical gyre. Ecosystems 2:181–214
Karl D, Letelier R, Hebel D, Tupas L, Dore J, Christian J, Winn C (1995) Ecosystem changes in the north Pacific subtropical gyre attributed to the 1991–92 El Niño. Nature 373:230–234
Karoly DJ, McIntosh PC, Berrisford P, McDougall TJ, Hirst AC (1997) Similarities of the Deacon cell in the Southern Ocean and Ferrel cells in the atmosphere. Q J Roy Meteor Soc 123:519–526
Killworth PD (2001) Rossby waves. In: Steele JH, Turekian KK, Thorpe SA (eds) Encyclopedia of ocean sciences. Academic Press, pp 2434–2443
Klein B, Roether WR, Manca BB, Bregant D, Beitzel V, Kovacevic V, Luchetta A (1999) The large deep water transient in the Eastern Mediterranean. Deep-Sea Res Pt I, 46, 371–414
Knap A, Jickells T, Pszenny A, Galloway J (1986) Significance of atmospheric-derived fixed nitrogen on productivity of the Sargasso Sea. Nature 320:158–160
Ledwell JR, Watson AJ, Law CS (1993) Evidence for slow mixing across the pycnocline from an open-ocean tracer-release experiment. Nature 364:701–703
Lee M-M, Williams RG (2000) The role of eddies in the isopycnic transfer of nutrients and their impact on biological production. J Mar Res 58:895–917
Lee M-M, Marshall DP, Williams RG (1997) On the eddy transfer of tracers: advective or diffusive? J Mar Res 55:483–505
Lévy M, Mémery L, Madec G (1998) The onset of a bloom after deep winter convection in the northwest Mediterranean sea: mesoscale process study with a primitive equation model. J Marine Syst 16:7–21
Lévy M, Klein P, Treguier A-M (2001) Impact of sub-mesoscale physics on production and subduction of phytoplankton in an oligotrophic regime. J Mar Res 59:535–565
Lewis MR, Harrison WG, Oakley NS, Hebert D, Platt T (1986) Vertical nitrate fluxes in the oligotrophic ocean. Science 234:870–873
Macdonald AM (1995) Oceanic fluxes of mass, heat and freshwater: a global estimate and perspective. PhD. thesis, Massachusetts Institute of Technology/Woods Hole Oceanographic Institute Joint program, Cambridge MA, 326 pp
Macdonald AM (1998) The global ocean circulation: a hydrographic estimate and regional analysis. Prog Oceanogr 41: 281–382
Macdonald AM, Wunsch C (1996) An estimate of global ocean circulation and heat fluxes. Nature 382:436–439
Mahadevan A, Archer D (2000) Modelling the impact of fronts and mesoscale circulation on the nutrient supply and biogeochemistry of the upper ocean. J Geophys Res 105:1209–1225
Marshall D (1997) Subduction of water masses in an eddying ocean. J Mar Res 55:201–222
Marshall J, Schott F (1999) Open-ocean convection: observations, theory and models. Rev Geophys 37:1, 1–64
Marshall JC, Nurser AJG, Williams RG (1993) Inferring the subduction rate and period over the North Atlantic. J Phys Oceanogr 23:1315–1329
Martin JH, Fitzwater SE (1988) Iron deficiency limits phytoplankton growth in the north-east Pacific subarctic. Nature 331: 341–343
McCartney MS (1977) Subantarctic mode water. In: Angel MV (ed) A voyage of discovery: George Deacon 70th anniversary volume. Deep-Sea Res (suppl.) 103–119
McClain CR, Firestone J (1993) An investigation of Ekman upwelling in the North Atlantic. J Geophys Res 98:12327–12339
McGillicuddy DJ, Robinson AR (1997) Eddy-induced nutrient supply and new production in the Sargasso Sea. Deep-Sea Res Pt I 44:1427–1449
McGillicuddy DJ, Robinson AR, Siegel DA, Jannasch HW, Johnson R, Dickeys T, McNeil J, Michaels AF, Knap AH (1998) New evidence for the impact of mesoscale eddies on biogeochemical cycling in the Sargasso Sea. Nature 394:263–266
McIntosh PC, McDougall TJ (1996) Isopycnal averaging and the residual mean circulation. J Phys Oceanogr 26:1655–1660
Menzel DW, Ryther JH (1961) Annual variations in primary production in the Sargasso Sea off Bermuda. Deep-Sea Res 7:282–288
Michaels AF, Knap AH, Dow RL, Gundersen K, Johnson RJ, Sorensen J, Close A, Knauer GA, Lohrenz SE, Asper VA, Tuel M, Bidigare R (1994) Seasonal patterns of ocean biogeochemistry at the U.S. JGOFS Bermuda Atlantic Time-series Study site. Deep-Sea Res Pt I 41:1013–1038
Michaels AF, Olson D, Sarmiento JL, Ammerman JW, Fanning K, Jahnke R, Knap AH, Lipschultz F, Prospero JM (1996) Inputs, losses and transformations of nitrogen and phosphorus in the pelagic North Atlantic Ocean. Biogeochemistry 35:181–226
Moore JK, Doney SC, Kleypas JA, Glover DM, Fung I (2002) An intermediate complexity marine ecosystem model for the global domain. Deep-Sea Res Pt II 49:403–462
Munk WH (1966) Abyssal recipes. Deep-Sea Res 13:707–730
Munk WH, Wunsch C (1998) Abyssal recipes II: energetics of tidal and wind mixing. Deep-Sea Res Pt I 45:1977–2010
Murtugudde RG, Signorini SR, Christian JR, Busalacchi AJ, McClain CR, Picaut J (1999) Ocean color variability of the tropical Indo-Pacific basin observed by SeaWiFS during 1997–1998. J Geophys Res 104:18351–18366
Newton CW (1978) Fronts and wave distributions in Gulf Stream and atmospheric jet stream. J Geophys Res 83, 9:4697–4706
Nurser AJG, Zhang JW (2000) Eddy-induced mixed-layer shallowing and mixed-layer/thermocline exchange. J Geophys Res 105:21851–21868
Orsi AH, Whitworth T, Nowlin WD (1995) On the meridional extent and fronts of the Antarctic Circumpolar Current. Deep-Sea Res Pt I 42:641–673
Oschlies A (2002) Can eddies make ocean deserts bloom? Global Biogeochem Cy (in press)
Oschlies A, Garçon V (1998) Eddy-induced enhancement of primary production in a model of the North Atlantic Ocean. Nature 394:266–269
Pelegri JL, Csanady GT (1991) Nutrient transport and mixing in the Gulf Stream. J Geophys Res 96:2577–2583
Pelegri JL, Csanady GT, Martins A (1996) The North Atlantic nutrient stream. J Oceanogr 52:275–299
Philander SGH (1990) El Niño, La Nina and the Southern Oscillation. Academic Press, 293 pp
Pollard RT, Regier LA (1992) Vorticity and vertical circulation at an ocean front. J Phys Oceanogr 22:609–624
Pollard RT, Lucas MI, Read JF (2002) Physical controls on biogeochemical zonation in the Southern Ocean. Deep-Sea Res Pt II 49:3289–3305
Polzin KJ, Toole JM, Ledwell JR, Schmitt RW (1997) Spatial variability of turbulent mixing in the abyssal ocean. Science 276: 93–96
Rhines PB (2001) Mesoscale Eddies. In: Steele JH, Turekian KK, Thorpe SA (eds) Encyclopedia of ocean sciences. Academic Press, pp 1717–1729
Rintoul SR, Wunsch C (1991) Mass, heat, oxygen and nutrient fluxes and budgets in the North Atlantic Ocean. Deep-Sea Res Pt I 38:S355–S377
Rintoul SR, Hughes C, Olbers D (2001) The Antarctic circumpolar current system. In: Siedler G, Church J, Gould J (eds) Ocean circulation and climate. Academic Press, pp 271–300
Roether WR, Manca BB, Klein B, Bregant D, Georgopoulos D, Beitzel V, Kovacevic V, Luchetta A (1996) Recent changes in Eastern Mediterranean deep waters. Science 271:333–335
Sathyendranathan S, Longhurst RSA, Caverhill CM, Platt T (1995) Regionally and seasonally differentiated primary production in the North Atlantic. Deep-Sea Res Pt I 42:1773–1802
Schmitz WJ (1995) On the interbasin-scale thermohaline circulation. Rev Geophys 33:151–173
Siedler G, Church J, Gould J (eds) (2001) Ocean Circulation and Climate: Observing and Modelling the Global Ocean. Academic Press, 712 pp

Siegel DA, McGillicuddy DJ, Fields EA (1999) Mesoscale eddies, satellite altimetry and new production in the Sargasso Sea. J Geophys Res 104:13359–13379
Smith RL (1995) The physical processes of coastal ocean upwelling systems. In: Summerhayes CP, Emeis K-C, Angel MV, Smith RL, Zeitzchel B (eds) Upwelling in the ocean: modern processes and ancient records. John Wiley & Sons, New York, pp 39–64
Spall SA, Richards KJ (2000) A numerical model of mesoscale frontal instabilities; plankton dynamics – I, model formulation and initial experiments. Deep-Sea Res Pt I 47:1261–1301
Speer K, Rintoul SR, Sloyan B (2000) The diabatic Deacon cell. J Phys Oceanogr 30:3212–3222
Stommel H (1979) Determination of watermass properties of water pumped down from the Ekman layer to the geostrophic flow below. P Natl Acad Sci Usa 76:3051–3055
Strass VH (1992) Chlorophyll patchiness caused by mesoscale upwelling at fronts. Deep-Sea Res 39:75–96
Strass VH, Woods JD (1991) New production in the summer revealed by the meridional slope of the deep chlorophyll maximum. Deep-Sea Res 38:35–56
Sverdrup HU (1953) On conditions of the vernal blooming of phytoplankton. Journal du conseil international pour l'exploration de la mer 18:287–295
Taylor AH, Colebrook JM, Stephens JA, Baker NG (1992) Latitudinal displacements of the Gulf Stream and the abundance of plankton in the North-east Atlantic. J Mar Biol Assoc Uk 72: 919–921
Toggweiler JR, Carson S (1995) What are upwelling systems contributing to the ocean's carbon and nutrient budgets? In: Summerhayes CP, Emeis K-C, Angel MV, Smith RL, Zeitzschel B (eds) Upwelling in the ocean: modern processes and ancient records. John Wiley & Sons, New York, pp 337–360
Toggweiler JR, Samuels B (1995) Effect of Drake Passage on the global thermohaline circulation. Deep-Sea Res Pt I 42:477–500
Townsend DW, Cammen LM, Holligan PM, Campbell DE, Pettigrew NR (1994) Causes and consequences of variability in the timing of the spring phytoplankton blooms. Deep-Sea Res Pt I 41:747–765
Uz BM, Yoder JA, Osychny V (2001) Pumping of nutrients to ocean surface waters by the action of propagating planetary waves. Nature 409:597–600
Veronis G (1973) Model of the world ocean circulation: 1. Wind-driven, two-layer. J Mar Res 31:228–288
Visbeck M, Jones H, Marshall J (1996) Dynamics of isolated convective regions in the ocean. J Phys Oceanogr 26:1721–1734
Voorhis AD, Bruce JG (1982) Small scale surface stirring and frontogenesis in the subtropical convergence of the western North Atlantic. J Mar Res 40 (suppl.) 801–821
Williams RG (2001) Ocean subduction. In: Steele JH, Turekian KK, Thorpe SA (eds) Encyclopedia of ocean sciences. Academic Press, pp 1982–1992
Williams RG, Follows MJ (1998a) The Ekman transfer of nutrients and maintenance of new production over the North Atlantic. Deep-Sea Res Pt I 45:461–489
Williams RG, Follows MJ (1998b) Eddies make ocean deserts bloom. Nature, 'News and Views' 394:228–229
Williams RG, Spall MA, Marshall JC (1995) Does Stommel's mixed-layer 'Demon' work? J Phys Oceanogr 25:3089–3102
Williams RG, McLaren A, Follows MJ (2000) Estimating the convective supply of nitrate and implied variability in export production. Global Biogeochem Cy 14:1299–1313
Woods JD (1988) Mesoscale upwelling and primary production. In: Rothschild BJ (ed) Toward a theory of biological physical interactions in the World Ocean. Kluwer, pp 7–38
Wu J, Sunda W, Boyle EA, Karl D (2000) Phosphate depletion in the western North Atlantic Ocean. Science 289:759–762
Wunsch C (1999) The interpretation of short climate records, with comments on the North Atlantic and Southern Oscillations. B Am Meteorol Soc 80:245–255
Wunsch C (2001) Global problems and global observations. In: Siedler G, Church J, Gould J (eds) Ocean circulation and climate. Academic Press, pp 47–56
Wunsch C, Hu D, Grant B (1983) Mass, salt, heat and nutrient fluxes in the South Pacific Ocean. J Phys Oceanogr 13:725–753
Zenk W (2001) Abyssal currents. In: Steele JH, Turekian KK, Thorpe SA (eds) Encyclopedia of ocean sciences. Academic Press, pp 12–27